

OTS PRICE

XEROX

\$

MICROFILM

\$

8.10 ph

FACILITY FORM 502

N64-29693

(ACCESSION NUMBER)

86

(PAGES)

Cr-58666

(NASA CR OR TMX OR AD NUMBER)

(THRU)

(CODE)

17

(CATEGORY)

Final Report

INVESTIGATION OF SLIP-RING ASSEMBLIES

George C. Marshall Space Flight Center
Huntsville, Alabama

IIT RESEARCH INSTITUTE

Final Report

INVESTIGATION OF SLIP-RING ASSEMBLIES

5 March 1963 to 5 March 1964

Contract No. NAS8-5251
Control No. TP3-83367 (IF)
IITRI Project E6000

Prepared by

IIT RESEARCH INSTITUTE
Technology Center
Chicago, Illinois 60616

for

George C. Marshall Space Flight Center
National Aeronautics and Space Administration
Huntsville, Alabama
Attn: M-P and C-MP

IIT RESEARCH INSTITUTE

Final Report

INVESTIGATION OF SLIP-RING ASSEMBLIES

5 March 1963 to 5 March 1964

Contract No. NAS8-5251
IITRI Project E6000

This report was prepared by IIT Research Institute under Contract No. NAS8-5251, "Investigation of Slip-Ring Assemblies," for the George C. Marshall Space Flight Center of the National Aeronautics and Space Administration. The work was administered under the technical direction of the Propulsion and Vehicle Engineering Laboratory, Materials Division of the George C. Marshall Space Flight Center with Mr. J. C. Horton acting as project manager.

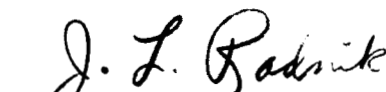
IIT RESEARCH INSTITUTE

FOREWARD

This is the Final Report of IITRI Project E6000, entitled, "Investigation of Slip-Ring Assemblies." The report covers the period 5 March 1963 to 5 March 1964.

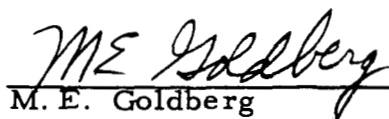
This program was conducted under the technical direction of J. L. Radnik. The project was administered by M. E. Goldberg, Manager, Reliability and Components Section. The cooperation of J. C. Horton and E. G. Lowe of the George C. Marshall Space Flight Center is gratefully acknowledged.

Respectfully submitted,
IIT RESEARCH INSTITUTE



J. L. Radnik
Assistant Manager
Reliability and Components Section

Approved by:



M. E. Goldberg
Manager
Reliability and Components Section



J. A. Granath
Associate Director
Electronics Research

IIT RESEARCH INSTITUTE

ABSTRACT

INVESTIGATION OF SLIP-RING ASSEMBLIES

29693

A laboratory investigation of miniature slip-ring assemblies was conducted to determine the influence of ring, brush and insulator materials on electrical noise and mechanical wear characteristics. Ring-brush material systems were evaluated by comprehensive laboratory tests of experimental slip-ring capsules. Insulation materials were evaluated by pyrolysis, liquid creep, and sublimation tests to establish contamination potential.

Electro-plated rings of soft gold and two hard gold alloys coupled with brushes of Neyoro 28A, a precious metal alloy, exhibited extremely low noise levels, particularly when tested in a drive apparatus that introduced a minimum of mechanical disturbance. Pyrolysis studies of epoxy resins indicated that the major gases given off at low temperatures were low molecular weight gases such as hydrogen, carbon monoxide and methane. No evidence of creepage or exudation of material from epoxy resins to adjoining metallic surfaces was obtained. Sublimation experiments indicated that condensible products were formed when epoxy resins were exposed to temperature gradients.

Author

TABLE OF CONTENTS

	<u>Page</u>
ABSTRACT	iv
I. INTRODUCTION	1
II. STATEMENT OF PROBLEM	2
III. PROGRAM OBJECTIVES AND SCOPE	3
IV. INSULATION COMPATIBILITY	5
A. Pyrolysis Studies by Gas Chromatography	6
B. Liquid Creep Characteristics	13
C. Sublimation Experiments	15
V. BRUSH AND RING MATERIALS	18
A. Ring Materials	18
B. Brush Materials	22
C. Experimental Capsules	22
VI. INSTRUMENTATION AND APPARATUS	30
A. Drive and Run-In Apparatus	30
B. Instrumentation	36
VII. LABORATORY EVALUATION-EXPERIMENTAL CAPSULES	43
A. General Noise Characteristics	43
B. Run-In Effects	61
C. Capsule Summaries	71
VIII. SUMMARY AND CONCLUSIONS	74
IX. RECOMMENDATIONS	76
X. CONTRIBUTING PERSONNEL AND LOGBOOKS	77

LIST OF TABLES

<u>Table</u>		<u>Page</u>
1	Gas Products of Thermal Stressed Teflon in Inert Atmosphere	8
2	Gas Products of Thermal Stressed Teflon in Air Atmosphere	9
3	Gas Products of Thermal Stressed Epon 828 in Inert Atmosphere	10
4	Resin Samples	11
5	Volatile Products from Pyrolysis of Resin Samples	12
6	Residues of Resin Samples after Pyrolysis at 900°C	13
7	Foil Creepage Tests	15
8	Sublimation Tests	17
9	Noise Measurements Comparison	48
10	Noise Transition Points	51
11	Noise Signature Data	54
12	Noise Signature Data	55
13	Effects of Continuous Rotation Run-In	64
14	Capsule Summaries	72

LIST OF FIGURES

<u>Figure</u>		<u>Page</u>
1	Sublimation Apparatus Assembly	16
2	Experimental Capsule Construction	24
3	Disassembled Experimental Capsule	25
4	Brush Block Fabrication Stages	26
5	Brush Block Fixtures	27
6	Brush Forming Jigs	29
7	Disassembled Drive Apparatus	31
8	Driving Arrangement - Torsional Drive	33
9	Noise and Deflection Instrumentation	38
10	General Laboratory Set-Up	39
11	Drag Torque Apparatus	40
12	Brush Force Apparatus	42
13	Double Frequency Character of Noise	44
14	Mechanical Loading Effects	46
15	RMS Noise Recordings Corresponding to Loading Effects of Figure 14	47
16	Noise Signatures	50
17	RMS Deflection and Noise During Free-Oscillation Test	53
18	Composite of Free-Oscillation Tests at Seven Stator Positions - Capsule 2-10	56
19	RMS Noise During Free-Rotation Test Capsule 2-17	58
20	Noise Oscillograms - Free Rotation Tests Capsule 2-17	59

LIST OF FIGURES (continued)

<u>Figure</u>		<u>Page</u>
21	Noise Oscillograms - 100 Hour Run-In Capsule 2-10	62
22	Noise Oscillograms - Capsule 2-17 Run-In	65
23	Photomicrographs - Capsule 2-17 After Run-In	67
24	Photomicrographs - Capsule 2-17 After Run-In	68
25	Photomicrographs - Capsule 2-17 After Run-In	69
26	Free-Oscillation Test - Capsule 2-17 After Run-In and Cleaning	70

INVESTIGATION OF SLIP-RING ASSEMBLIES

I. INTRODUCTION

This report summarizes the results of a laboratory investigation conducted during IITRI Project E6000, "Investigation of Slip-Ring Assemblies," for the George C. Marshall Space Flight Center, National Aeronautics and Space Administration, Huntsville, Alabama. The program was concerned primarily with the evaluation of appropriate materials for miniature slip-ring assemblies operating in a dry nitrogen environment.

Slip-ring assemblies are normally used to transmit electrical information across the axes of inertial platforms in space vehicle guidance systems. Since many of the circuits are null-seeking circuits, it is imperative that the brush-ring combination maintain uniform, low noise contact in the low level or dry circuit area.

The investigation described herein was specifically directed toward problem areas encountered with a 80 ring capsule used in launch vehicles. This capsule is described in Drawing GC-125209, entitled "Specifications for ST-124 Slip-Ring Assemblies," issued by the George C. Marshall Space Flight Center, Astrionics Laboratory. The capsule must be capable of complete 360° rotation even though its normal oscillation about a fixed operating point is only about 0.5 minutes of arc. Its operating life in a launch vehicle is only about 2 minutes, but qualification and acceptance tests require a total life of about 75 hours. For the laboratory work of this program, experimental capsules were fabricated having the same ring and brush dimensions as the actual capsule in order to simulate the actual operating conditions as closely as possible.

II. STATEMENT OF PROBLEM

The two general problem areas associated with miniature slipping operation are excessive electrical noise and inadequate wear characteristics. Excessive electrical noise at the sliding contact strongly interferes with circuit performance, particularly the null-seeking type. Inadequate wear characteristics limit the operating life and restrict the extent of check-out. In some instances, deep wear tracks are obtained after relatively short operating times. In other instances, a stick-slip phenomena is encountered which sometimes leads to fracture of brush wipers.

Electrical noise at the sliding contact is dependent on many inter-related factors including materials, surface finishes, contaminant films, wear debris, etc. Wear characteristics are generally determined by the mechanical properties of the ring and brush materials, surface conditions, brush forces, and presence of lubricant films.

The two problem areas are somewhat interdependent since inadequate wear characteristics generally result in large deposits of wear debris which then produce extremely high noise levels. Conversely, a high initial noise level generally indicates a poor surface condition, a condition which leads to accelerated wear effects.

III. PROGRAM OBJECTIVES AND SCOPE

The principal objective of this program was the evaluation of candidate slip-ring and insulator materials for the purpose of specifying materials that would permit improvements in the performance of miniature slip-ring assemblies. The evaluation of materials was approached only from the performance view-point although it is recognized that factors such as fabrication adaptability and cost justifiably influence the eventual selection of materials. Most candidate materials were selected, however, from materials which are or could be used in commercial slip-ring assemblies.

The investigation of slip-ring characteristics was divided into three basic tasks. Since there is a possibility that gases or condensable material produced by organic polymeric components could greatly accelerate wear and objectionable noise characteristics, one of the tasks was devoted to a laboratory analysis of the compatibility of insulator materials. Dielectric material is used for the ring body, the brush blocks, and also for insulation of the individual lead wires.

The second task of the program was concerned with the development of apparatus and instrumentation for complete evaluation of experimental capsules. This included the design and fabrication of a drive mechanism for testing capsules under conditions of oscillatory motion, continuous rotation, and combinations thereof. It also included assembly of instrumentation for electrical noise, contact resistance, drag-torque and brush force measurements. In addition, laboratory apparatus for various "run-in" conditioning processes was also developed.

The third task of the program was devoted to the laboratory evaluation of experimental capsules. Experimental capsules were fabricated with various ring-brush material combinations in a configuration which closely simulated the constructional features of an actual 80 ring capsule. Both the initial and the after "run-in" performance characteristics were established in order to permit comparisons of material dependent factors.

IV. INSULATION COMPATIBILITY

Contaminant films on the contacting surfaces resulting from degradation of insulating components could be prime contributors to the high noise level and short wear life inadequacies of assemblies. Polymeric components are, by their very nature, prime suspects in malfunctions caused by contaminant films.

Plastic components originate from low-molecular weight materials which are caused to combine with one another by heating and/or introduction of catalysts. Ideally, the product consists entirely of high molecular weight solid, non-volatile polymeric molecules with no mobile components. In practice, this is approached but never completely fulfilled; traces of low molecular weight impurities and sometimes very small amounts of unreacted monomer will remain imbedded in the polymeric mass. Although some of the impurities may be eliminated during the curing process, some will be retained and will subsequently diffuse to the surface over a relatively long time period. These materials can migrate to the contact surfaces by a process of thermal diffusion involving evaporation from the plastic surface and condensation on the ring surface. Temperature differentials will strongly promote such transfers.

Another conceivable mode of migration of organic materials is the wetting action by a liquid exudate from the polymer on a metal surface with which it is in direct contact. By either the thermal diffusion or liquid exudate mode of migration, contaminant materials may result on the contact surfaces where they can be converted to less volatile, solid materials by frictional and thermal effects.

The contamination potential of candidate insulating materials was determined by a study of pyrolysis, liquid creep, and sublimation characteristics of materials that are or could be used in present slip-ring designs. Ceramic materials were not evaluated principally because of their incompatibility with molding and machining operations required in miniature assemblies.

A. Pyrolysis Studies by Gas Chromatography

1. Method

To establish the thermal stability of candidate materials, samples were subjected to higher than normal thermal stresses and the amount and chemical nature of gases produced were determined by gas chromatography. At suitable temperature intervals, off-gases produced from the sample were swept out of the pyrolysis chamber into the gas chromatography separation column by an inert gas such as helium. The pyrolysis oven was essentially a U-shaped tube with the sample placed at the bottom and with a thermocouple inserted in a well just above the sample to determine temperature. The gas used to flush out the gaseous products was passed into one arm and out the other and then directly into the gas chromatograph column. The separation columns were 18 and 30 foot lengths of 1/4 inch tubing packed with 40-60 mesh Chromosorb W coated with 20 percent Kel-F oil. The columns were installed on a Burrell K-1 gas chromatograph using a thermal conductivity detector.

The pyrolysis tests were basically attempts to study the volatility of the products given off at boiling point temperatures from about 30 to 200°C by determination of the amount of material given off at various

pyrolysis temperatures. Analysis of the distribution of gas decomposition products then permitted a qualitative evaluation of the thermal stability of the material. From an insulation compatibility viewpoint, the best insulator material is one which is least likely to produce reactive gases since these gases could eventually lead to noise and wear problems.

2. Experimental Results - Pyrolysis Studies

The initial pyrolysis experiments were performed with samples of Teflon both in an inert atmosphere (helium) and in an air atmosphere. The component gases given off were identified by infrared spectroscopy and the amounts of each component and also the total amounts of gas evolved were calculated from the gas chromatograms of the pyrolysis gases. Table 1 is a summary of the pyrolysis products of Teflon in an inert atmosphere and Table 2 is the corresponding summary for an air atmosphere. Comparison of data indicates that there is almost twice as much total gas given off in air as in an inert gas atmosphere. This suggests that air may be acting as a catalyst in promoting off-gassing. The data also shows that the reactive gas C_2F_2 is given off only in the presence of air.

After completion of the Teflon tests, further pyrolysis tests were conducted only in an inert gas atmosphere since it was established that capsules are operated only in a dry nitrogen atmosphere. Table 3 summarizes the results of pyrolysis studies of an aromatic amine-cured resin of Epon 828. As indicated, the major gases given off in the 700°C to 900°C range were hydrogen and methane. High boiling point components were also indicated by condensation of a brown viscous liquid in stop-cocks and metal tubing used for the delivery of the gas samples to the gas chromatograph column.

Table 1

GAS PRODUCTS* OF THERMAL STRESSED TEFLON IN INERT ATMOSPHERE

Pyrolysis T °C	Peak 1 CF ₄	Peak 2 C ₂ F ₄	Peak 3 nC ₃ F ₆	Peak 4 Cyclo C ₄ F ₈	Peak 5 Iso C ₄ F ₈	Peak 6 Unknown	Total Gas STP .01 g Resin in μ l
300	0.24	0.61			0.65		0.33
400	2.35	2.9			2.07		1.64
460	1.98	6.75	0.32		2.06		2.50
490	8.20	71.8	6.25	7.85	5.27		22.7
515	21.7	184	22.3	92.2	9.75		74.1
535	62.7	258	84.5	461	8.06	8.06	198
555	116	415	235	822	22.6	31.2	369
574	260	532	471	1430	52.0	58.5	629
594	288	271	107	155	12.9		187
617	19.3	16.0	4.8	7.1	25.3		16.3
Total	780.47	1758.06	931.17	2975.15	204.01	97.76	

* All figures given are in moles $\times 10^{-8}$ per .010 g of resin.

Table 2

GAS PRODUCTS* OF THERMAL STRESSED TEFLON IN AIR ATMOSPHERE

Pyrolysis T°C	CF ₄	C ₂ F ₆	C ₂ F ₄	C ₂ F ₂	Cyclo C ₄ F ₈	Unknown Peaks of Higher Boilers	Total Gas STP .010 g. Resin in ul
300	Trace		Trace				
400	4.4		4.2				1.9
450	4.4		4.2		0.2	1.8	2.4
495	23.8		73.8		7.4		23.5
525	252	126	956	13	65	26	322.0
550	244	972	1202	342	1340	125	947.0
567	207	1030	1240	700	1360	276	1080
596	111	36.2	258	12	18	24	102.0
Total	946.6	2164.2	3738	1067	2790.6	452.8	2399.8

* All figures are given in moles x 10⁻⁸ per .01 g. of resin.

Table 3

GAS PRODUCTS* OF THERMAL STRESSED EPON 828
IN INERT ATMOSPHERE

Pyrolysis ToC	H ₂	CO ₂	CO	CH ₄	C ₂ H ₄	C ₂ H ₆	C ₃ H ₆	C ₃ H ₈
200			13					
300		4	18					
400		45	124		13	22	13	
500	23	45	563		112	153	117	50
600	62	45	855		172	178	128	44
700	838	32	2110		210	126	66	34
800	1060		5510		142	54	22	
900	3270		5430					

* All figures are given in moles x 10⁻⁸ per 0.01 g of resin.

Pyrolysis studies were also conducted with four other epoxy resins having various hardener and filler additions. These resins are identified in Table 4. Data on the volatile products from these resins is shown in

Table 4
Resin Samples

<u>Sample</u>	<u>Resin</u>	<u>Hardener</u>	<u>Filler</u>
ES 84	Epon 828	Z	None
ES 134	DER332	Z	None
ES 137	DEN438	NMA	Li Al SiO ₂
P 51	Epon 828	V-125	None

Table 5. The data shown was summarized from more detailed information in order to present an over-all indication of the volatility. The number of different peaks indicated on the gas chromatograms is shown in parentheses following the figures. The table indicates that the pyrolysis behavior of ES84, ES134 and P51 is roughly similar in that major quantities of volatiles are given off in the 600°C to 900°C range with no detectable gas evolution below 500°C. ES137, a sample containing an inert filler material, was found to produce gas at 400° and 500°C. Since the actual resin content of sample ES137 is approximately one-half that of the other three samples, the quantities shown in Table 5 for ES137 should be doubled to obtain relative comparisons.

The amounts of residue obtained from the four resins after pyrolysis at 900°C were also determined. These residues are the material remaining after pyrolysis at the final temperature of 900°C. Table 6

Table 5

Volatile Products from Pyrolysis of Resin Samples
(Millimoles $\times 10^{-8}$ per 0.01 gram of sample)

Resin Sample	Approx. B.P. of Volatiles	Pyrolysis Temp.					
		400C	500C	600C	700C	800C	900C
ES84	below 35C			93	3403	3014	403
	35 - 200C			21	133(3) ^b	262(2)	106(2)
	over 200 C+H ₂ O ^a				1235(2)	853(2)	140
ES134	below 35C		122	1280	772	3600	2970
	35 - 200C				124(2)	536(3)	944(3)
	over 200C+H ₂ O			1200	660	2942	1158
ES137	below 35C	18	78	355	3635	665	361
	35 - 200C	341(2)	534(2)	510	840(2)	160(3)	69(3)
	over 200C+H ₂ O				1651	38	66
P51	below 35C		32	319	4020	6040	3440
	35 to 200C		72(2)	236(5)	671(3)	1258(3)	681(3)
	over 200C+H ₂ O		128	300	2030	1523(3)	202

a. Mostly water

b. Figures in parentheses show number of gas chromatographic peaks obtained.

Table 6

Residues of Resin Samples after Pyrolysis at 900°C

<u>Resin</u>	<u>% Residue (by weight)</u>	
ES 84	1.6	3.6
ES 134	12.1	10.0
ES 137	57.6	58.0
P 51	9.3	8.8

summarizes the residue data for two different runs which were conducted several weeks apart. The data gives an indication of the reproducibility of the pyrolysis experiments.

B. Liquid Creep Characteristics

1. Methods

The general approach taken to determine liquid creep characteristics was to place a strip of gold foil in contact with an insulation sample and determine weight changes of the foil and the sample after exposure to high temperatures for extended time intervals. The foil was also examined under a microscope to determine creepage. A sealed glass chamber was constructed from two sections of glass tubing approximately 3 inches in diameter with a large ground joint in the middle. Gas inlet and outlet ports were provided to permit sampling of any off gases during exposure to various test temperatures. Initial interference from stop-cock grease was avoided by using a narrow strip of teflon sealing tape on the dry ground joint before sealing.

2. Experiment Results - Liquid Creep Studies

The initial liquid creep experiments were performed at 100°C and 200°C for periods up to seven days with samples of cured Epon 828 and Epon 1009, but no evidence of creepage was obtained. No gain in weight of the gold foil was detected even though the resin lost up to 30 percent in weight. Most of this loss was apparently associated with gas evolution.

The following method of inducing creepage was also tried; a glass slide was coated with Epon 1009 by melting some of the powdered resin on a hot plate and letting it spread over the surface of the slide. A strip of gold foil was then mounted forming a sandwich, the resin in the middle. By means of a split cork stopper, the sandwiched portion was sealed within a test tube in such a manner that the foil protruded outside the stopper. The gold foil was then placed in contact with a knife heater and heated to 100°C for three days. It was found that the gold foil adhered to the resin on the slide. The foil could be pulled off easily however and showed no gain in weight. The slide and resin were re-weighed and showed no loss in weight.

In a similar experiment using a thin sliver of cured Epon 828 resin, no adhesion between resin and foil was found. Also in this case, no weight changes were found for the gold foil and the glass slide.

Table 7 summarizes the results of similar creep experiments with the four modified epoxy resins described in Table 4. In general, no evidence of creepage was obtained in the foil experiments, and therefore, further experiments were not performed.

Table 7
Foil Creepage Tests

<u>Resin Sample</u>	<u>Sample Size</u>	<u>Test Temperature</u>	<u>Results</u>
ES 84	53 mg.	72 hrs at 100°C	No weight change
ES 134	46 mg.	72 hrs at 100°C	No weight change
ES 137	87 mg.	72 hrs at 100°C	No weight change
P 51	35 mg.	72 hrs at 100°C	No weight change

C. Sublimation Experiments

1. Method

Contamination potential of insulating materials was also determined by establishing whether any material given off by an insulation sample would condense on the cold finger of a sublimation apparatus. A glass sublimation cell was set up as shown in Fig. 1. A hot plate was used to heat a sand bath which was kept in contact with the outside shell of the sublimation apparatus. The insulation sample was packed down in contact with the inside of the sublimation cell. The cold finger was supplied with coolant from a cold bath maintained between -10°C and -20°C. A vacuum pump was attached to the head space through a U-trap immersed in a dry-ice bath. The vacuum was less than 1 mm but was not measured although it was sustained for the entire duration of the experiment. Each run was performed at 200°C for 72 hours after which weight loss of the sample was determined.

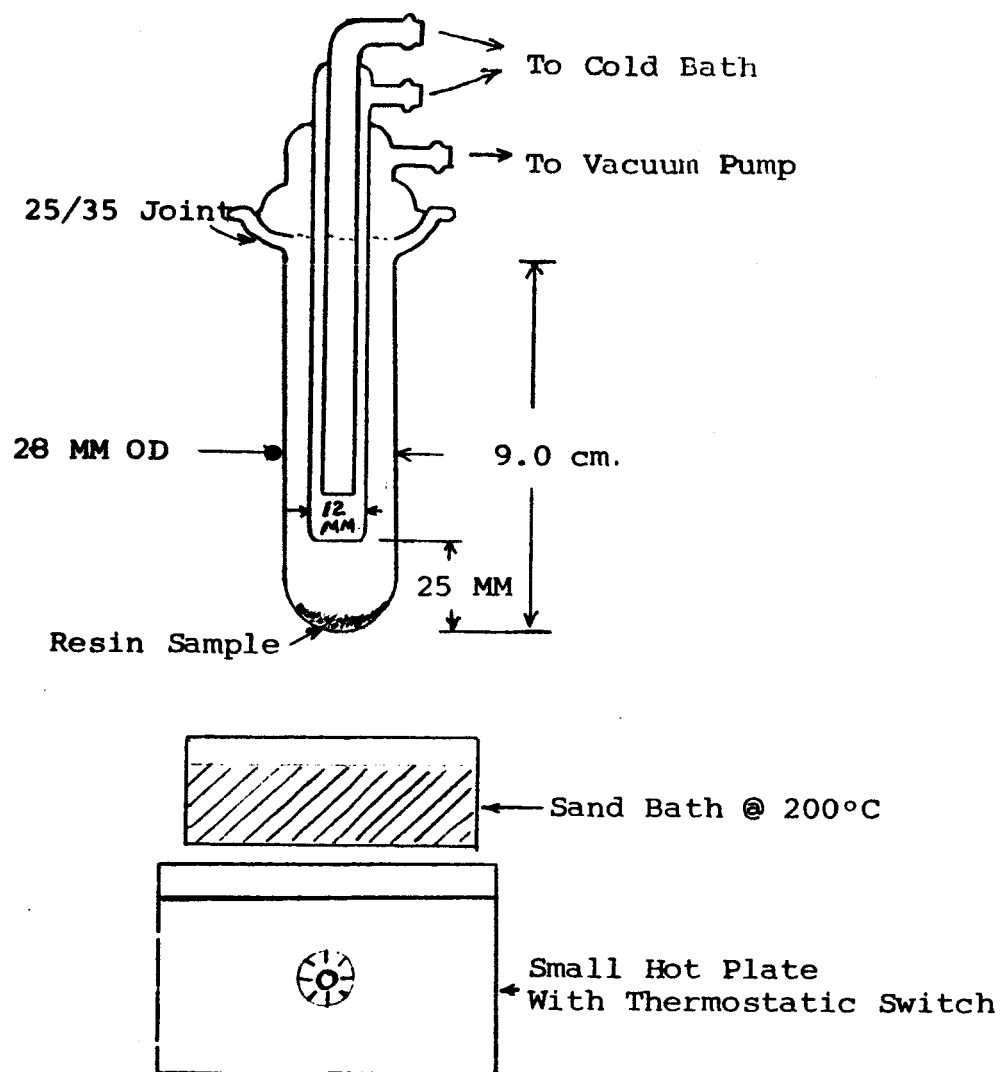


Figure 1
 SUBLIMATION APPARATUS ASSEMBLY
 IIT RESEARCH INSTITUTE

2. Experimental Results - Sublimation Studies

The sublimation experiments were performed with the four modified epoxy resin samples described in Table 4. The data and observation resulting from these experiments are presented in Table 8. In each of the three cases

Table 8
Sublimation Tests

<u>Resin Sample</u>	<u>Test Conditions</u>	<u>Weight of Sample, mg</u>	<u>Weight of Loss, mg</u>	<u>% Loss</u>	<u>Remarks</u>
ES 84	72 hrs at 200°C	146.2	9.6	6.6	Light amber condensate
ES 134	72 hrs at 200°C	155.2	16.8	10.8	Carmine-red condensate
ES 137	72 hrs at 200°C	125.9	5.1	4.0	No apparent condensate
P 51	72 hrs at 200°C	111.	11.6	10.4	Orange-red condensate

where condensate was noted, it appeared in about 25 to 30 hours. As indicated, there was no apparent condensate for the filled epoxy sample, ES 137. In each of the runs, there was a very small amount of clear liquid condensed in the dry ice trap but this evaporated very shortly after exposure of the trap to room temperature. The sublimation residue samples from ES 84 and P 51 became somewhat lighter in color while ES 137 became slightly darker. Sample ES 134 apparently lost part or all of its dye and turned from a red to a buff color.

V. BRUSH AND RING MATERIALS

The basic requirements for brush and ring materials in miniature slip-ring assemblies are somewhat contradictory in that soft, non-reacting materials such as the noble metals are required for low resistance, low noise contacts while hard, low coefficient of friction materials are required for good wear and mechanical properties. Consequently, the selection of appropriate brush and ring materials entails an engineering compromise in which the divergent requirements are satisfied to the fullest over-all extent possible. The selection of materials is also influenced by fabrication requirements and cost. Although the latter factors were not considered in this investigation, their importance is fully recognized.

A. Ring Materials

Because of the importance of low noise sliding contacts, particularly in null-seeking circuits, the ring materials selected for evaluation were chosen primarily for their non-reacting nature. Additional consideration was also given to mechanical characteristics. The ring materials evaluated were soft gold, soft gold with hard gold overlays, rhodium, and a gold-graphite composite.

Experimental rings were formed by electro-deposition on a leaded brass cylinder 0.264 in. OD x 0.445 in. long x 0.007 in. wall thickness. After plating, four vee grooves spaced on 1/16 in. centers were machined in the center section of the cylinder.

A cleaning operation was required for the leaded brass cylinders prior to the plating operation in order to obtain good massive deposits. The following cleaning procedure was found to be effective in providing a clean, platible surface:

- a) Soak and brush lightly in first benzene dip, dry in air
- b) Soak in second benzene dip for about 15 seconds, air dry
- c) 10-20 second etch in 20 percent fluoboric acid (HBF_4),
water rinse
- d) Electroclean in sodium orthosilicate (100grams/liter) 190°F ,
10 seconds at 8 volts, specimen cathodic, water rinse
- e) Re-etch in 20 percent HBF_4 for about 10 seconds, water
rinse
- f) Immediately introduce specimen into bath with bath energized
to minimize immersion plating effects.

The following plating baths were utilized to obtain experimental ring samples:

a) Soft Gold

Soft gold coatings were obtained from the Orotemp 24K bath, a 24K neutral gold formulation supplied by Technic, Inc., Providence, R.I. This bath is a proprietary, high cathode efficiency, neutral bath (pH 5.0-7.0) which produced dense, sound soft deposits. The bath was operated at about 140°F and a terminal voltage of 2.0 volts. Current density was 25.8 amps per square foot (asf) and the cathode efficiency averaged 93 percent. The electro-plates obtained from this bath had a hardness of 55-60 on the Vickers 15 gram micro-hardness scale.

b) Hard Gold "A"

Hard Gold "A" was one of two overlay materials evaluated as a 100 micro-inch flash over soft gold. Hard Gold "A" was electro-deposited from the Orotherm HT bath, a proprietary acid-type, bright

gold bath supplied by Technic, Inc. The bath was operated at about 110°F and the voltage was 2.25 volts. The cathode efficiency of the Orotherm HT bath was 31.8 percent.

c) Hard Gold "B"

Hard Gold "B" overlays were obtained from the Autronex NI bath, an acid-type bright gold formulation supplied by Sel-Rex Corporation, Nutley, New Jersey. The 100 micro-inch flash was plated from the bath operated at 110°F and a pH of 3.95. Cathode efficiency averaged about 42 percent.

d) Rhodium Bath

Rhodium plated rings were electro-deposited from an acid, rhodium sulfate bath of the following composition:

Rhodium Metal	20 grams/gal
Sulfuric Acid, conc.	50 ml/gal
Water	To make 1 gal.

The bath was operated at about 115°F at a current density of about 15 asf. An insoluble anode was employed, and it was necessary to make rhodium additions to the bath periodically. Cathode efficiency average 86.5 percent.

A brief investigation was also conducted on the use of precious metal hardening agents to obtain gold alloy deposits which may have higher corrosion resistance than the conventional hard golds. Alloying agents are used in gold baths to obtain deposition of the brighter, harder golds. The normally used agents are nickel, cobalt, indium or silver in trace amounts. It was hypothesized that corrosion problems with hard golds could result from the

diffusion to the surface of some of the hardening elements that possess inferior corrosion properties, as for example silver or nickel. It was further postulated that the use of non-reactive precious metals as hardening agents in gold plating baths would offset such a possibility. An attempt to investigate this concept was made by obtaining a high purity, alkaline, non-cyanide gold bath as the vehicle for possible additions. The formulation utilized was the Oro-verge B gold bath. Experimental work was performed to characterize the gold from this bath prior to the addition of the precious metal hardening agents. The bath was operated under many conditions of current density, temperature, and agitation, but good gold deposits could not be obtained. Some improvement was obtained when the bath was filtered in fine, activated charcoal after every run, but the plated gold was still rough and nodular in appearance. For this reason, further investigation of bath modification was not pursued.

One other plating approach was used in fabrication of experimental rings. A ring cylinder was plated from a soft gold bath containing a suspension of fine graphite particles. It was postulated that contact sticking or welding could be minimized by a gold plate in which fine graphite particles were suspended. It was reasoned that the continuous matrix of gold would be interrupted by the presence of fine graphite particles, thus producing a surface which would be less susceptible to welding or sticking. Examination of the composite plated cylinder with a 800X microscope did not indicate the presence of any discrete graphite deposits. However, since the graphite particles were of the order of 100 microns in diameter, they would be difficult to distinguish if they were finely dispersed in the gold layer. The experimental evaluation of the gold-graphite rings is described in a later section.

B. Brush Materials

A suitable brush material is one that is non-reacting and possesses good mechanical characteristics. Because of the small dimensions involved, the unit pressures are quite large, and a brush material which is relatively hard is desirable. Hertzian stress analysis, based on purely elastic deformation, indicated that the contact stress can be extremely high because of the small dimensions involved. Precious metal alloys are the most suitable because they combine the non-reacting properties of precious metals with the hardness properties that are characteristically obtained by alloying.

Two precious metal alloys have demonstrated general suitability for brush applications. These are Paliney No. 7 and Ney-Oro No. 28A. Paliney No. 7 is an alloy containing approximately 35 percent palladium, 10 percent platinum, 30 percent silver, 15 percent copper and 10 percent gold. Ney-Oro 28A is a 75 percent gold, 21.5 percent silver, and 3.5 percent nickel alloy which exhibits a good combination of conductivity, hardness and corrosion resistant properties. Experimental brushes were fabricated from both materials in accordance with the technical requirements of "Specifications for ST-124 Slip-Ring Assemblies," but because the tolerances specified in the referenced specification could be satisfied much more easily with Ney-Oro 28A, this material was used for the brushes in all experimental capsules.

C. Experimental Capsules

Candidate ring materials were evaluated by construction of experimental slip-ring capsules which simulated the standard 80 ring slip-ring assembly. The capsule was designed to accommodate the small ring cylinders upon which the candidate materials were plated. The experimental

capsule contained isolated Nooteboom brushes riding in 90° V grooves on the common ring cylinder. Noise and resistance measurements were made between pairs of brush leads.

Figure 2 shows the general construction of the experimental capsule along with an additional ring cylinder and brush block. Figure 3 is an exploded view of the experimental capsule showing the internal structural features. The bearings used in the experimental capsule were identical to those specified for the 80 ring capsule.

The experimental ring cylinders were machined with a special diamond tool that was shaped to produce the 90° V groove. Surface finishes of approximately No. 4 rms were obtained. After machining, all parts were cleaned by an ultrasonic process using an Alconox solvent. This procedure was later modified by cleaning in acetone and then rinsing with distilled water.

Perhaps the most delicate operation in the fabrication of the experimental capsule was the assembly of the brush block. The brush block was machined from a bakelite tube, and the four brushes were cemented in place along a groove in the back surface of the brush block. Figure 4 shows the bakelite brush block in various machining stages along with several fixtures used in the machining operations. Figure 5 illustrates a fixture that was used to install the completed brush block in a capsule without damaging the brush wipers. The other fixture shown in Fig. 5 was used to hold the brush block during the drilling of the four corner holes by which the block is secured in the capsule.

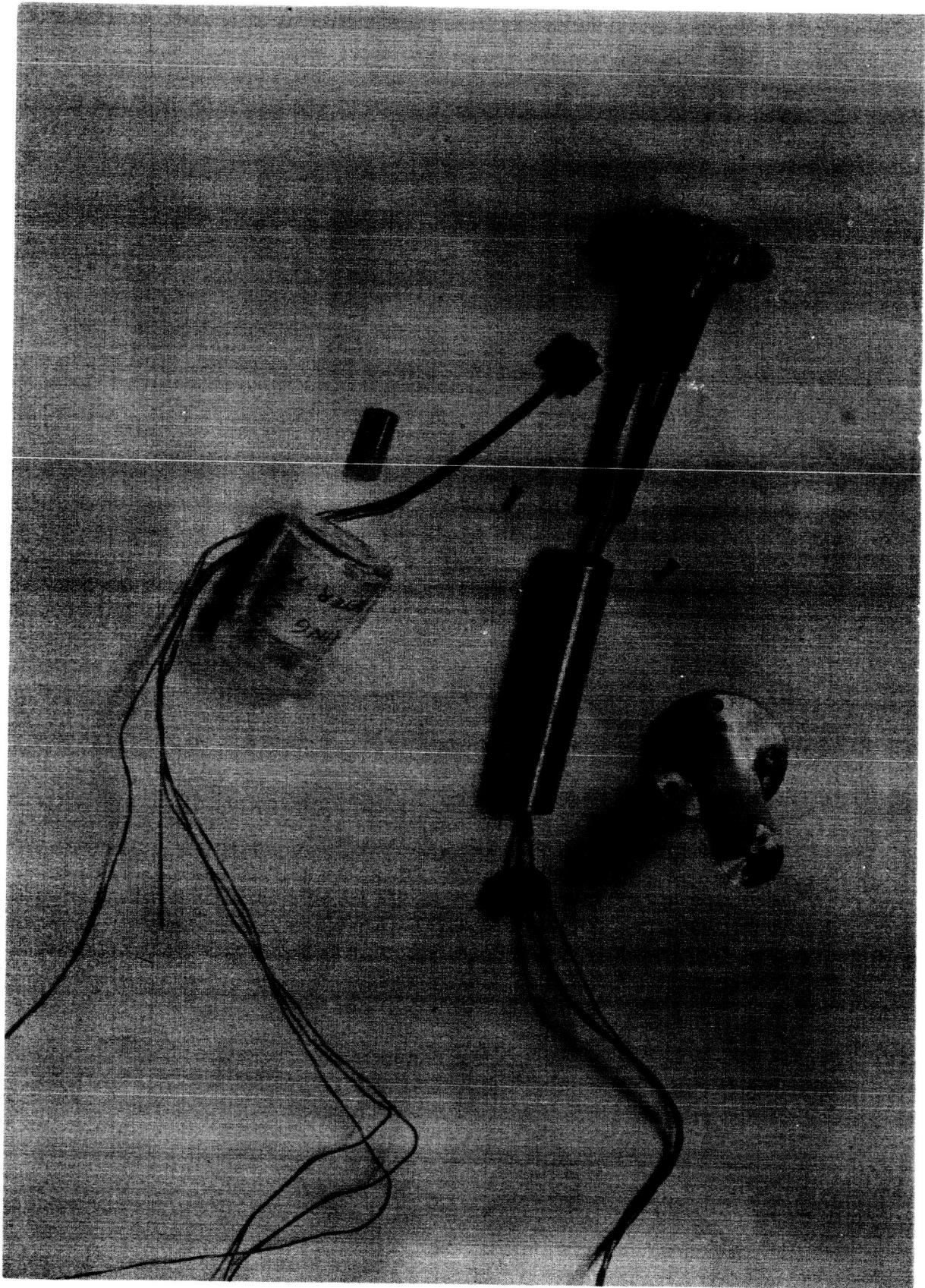


Fig. 2: EXPERIMENTAL CAPSULE CONSTRUCTION

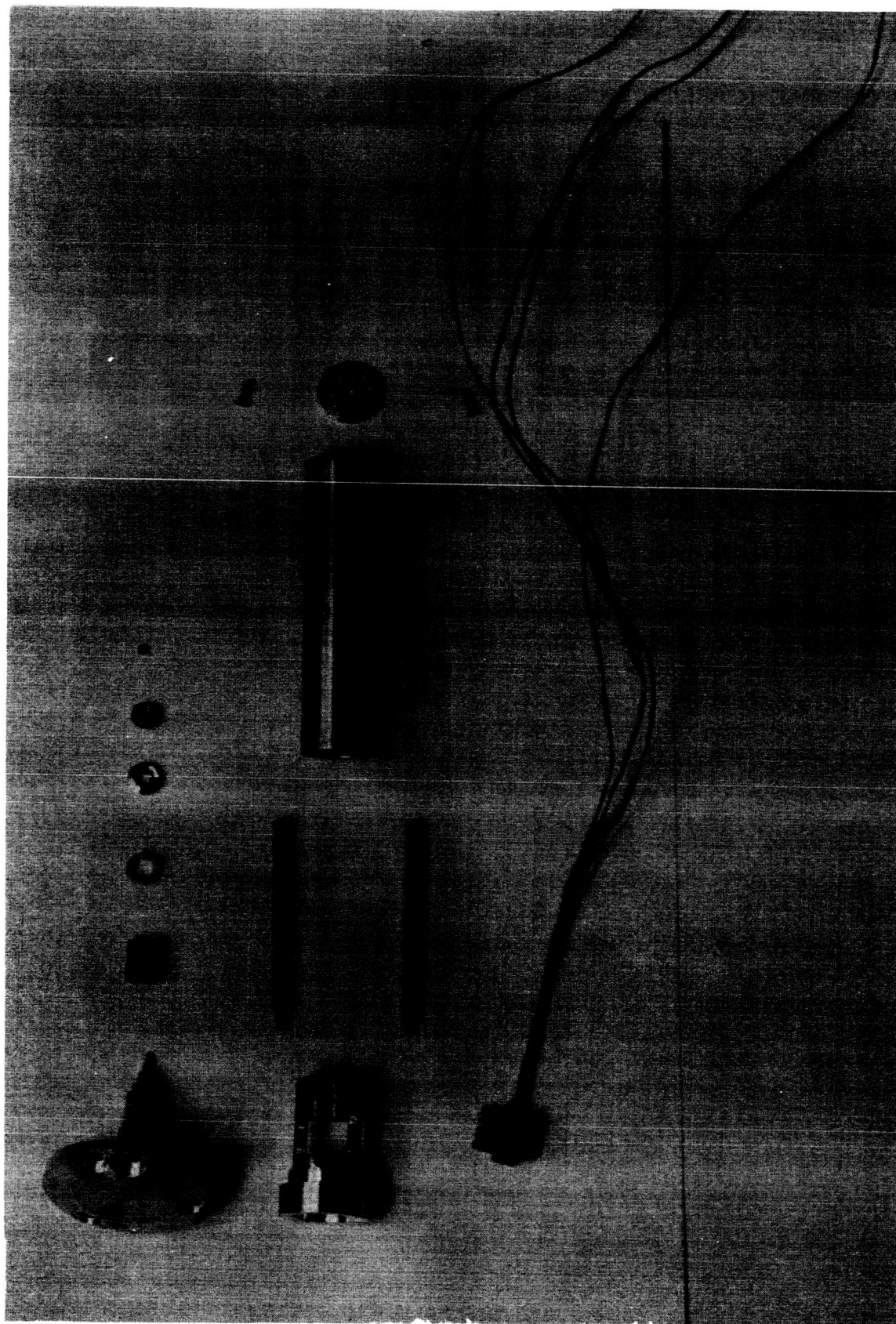


Fig. 3: DISASSEMBLED EXPERIMENTAL CAPSULE

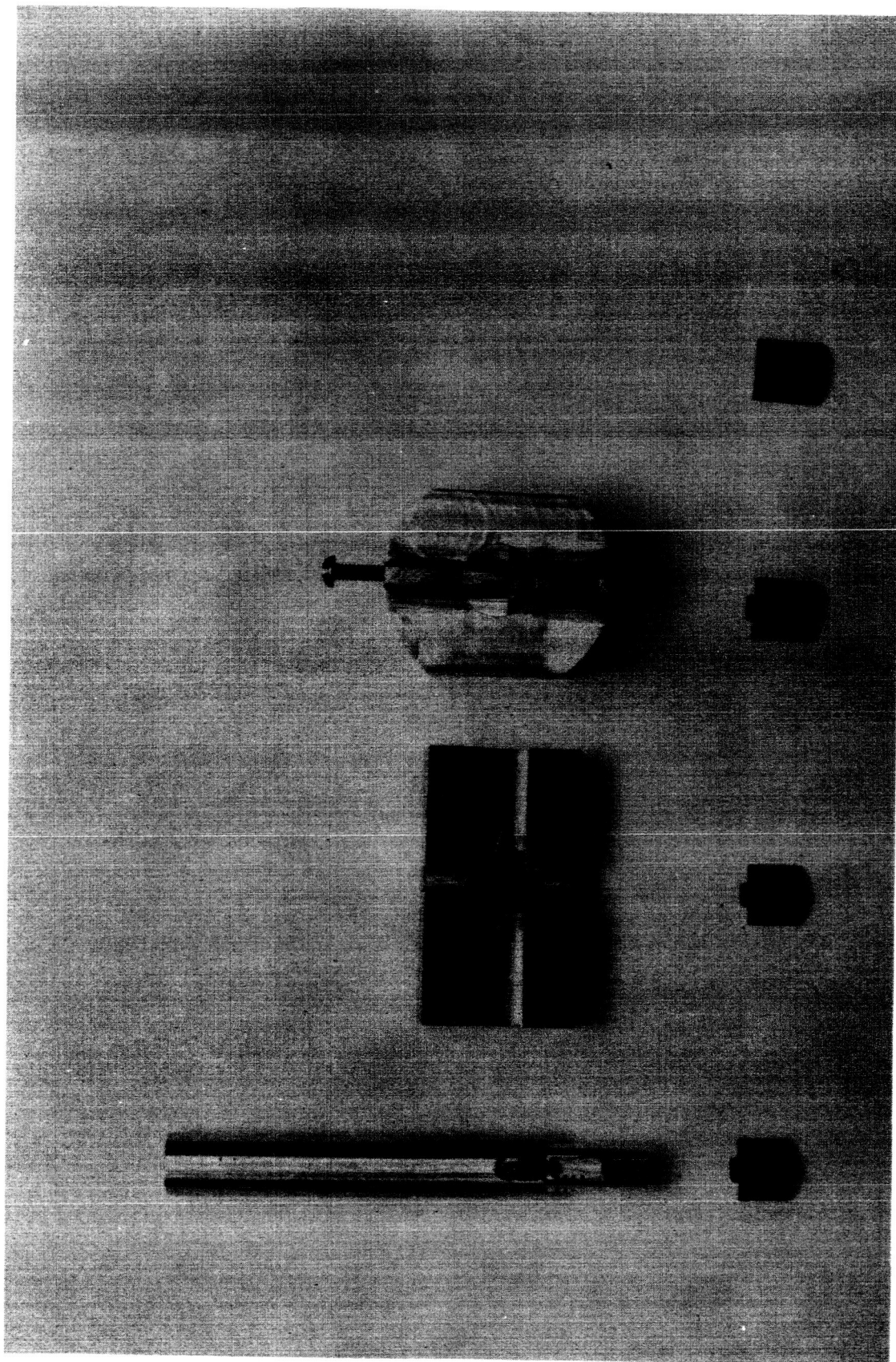


Fig. 4: BRUSH BLOCK FABRICATION STAGES

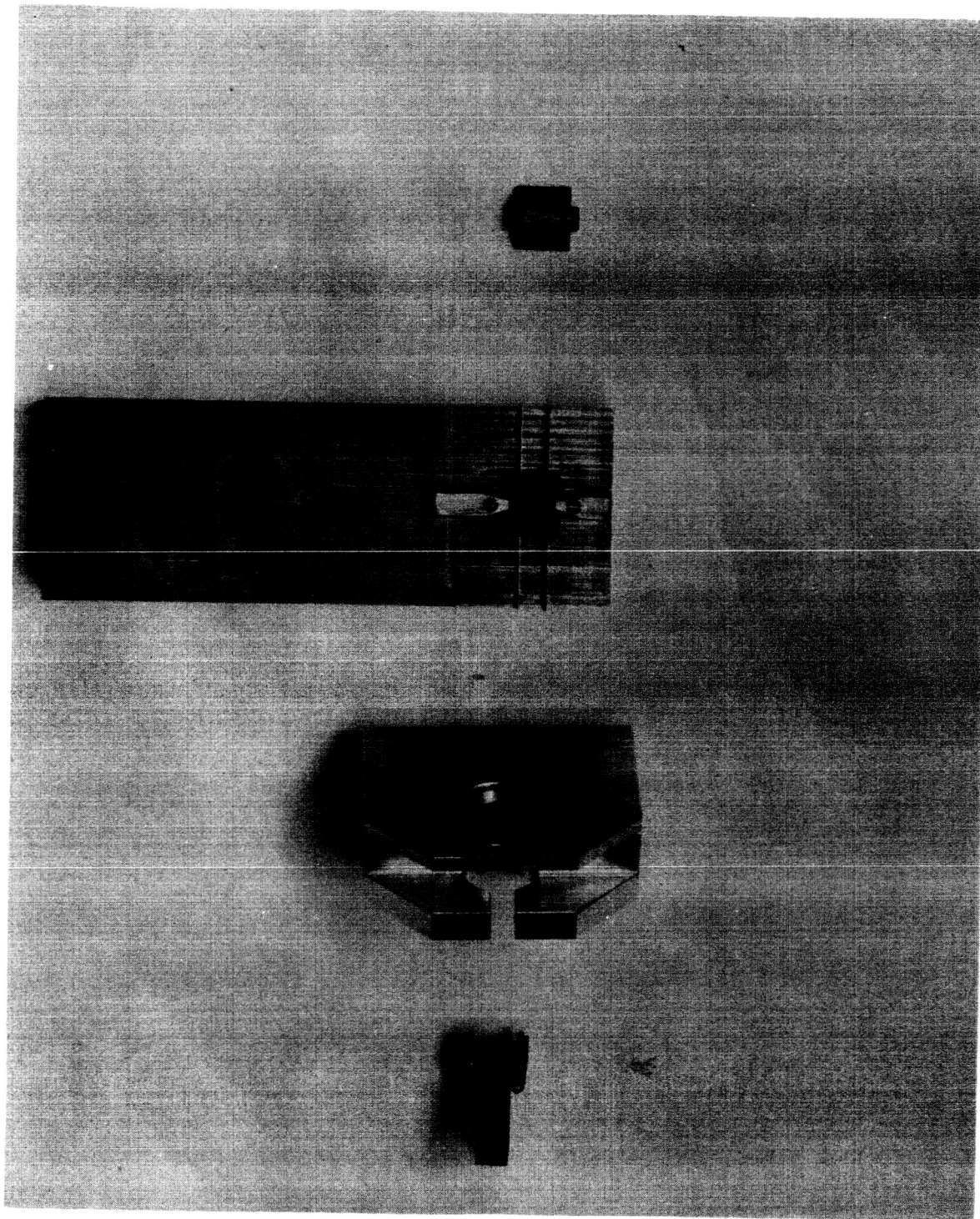


Fig. 5: BRUSH BLOCK FIXTURES

Figure 6 shows the jigs that were used to form the Nooteboom brushes from cold worked Ney-Oro 28A, 7 mil diameter wire. Special precautions were observed to avoid die marks on the brush surface during forming. Thirty inch lengths of the lead wire specified in Astrionics Labroatory Drawing No. GC-125209 were soldered to each brush along the back edge before cementing to the brush block.

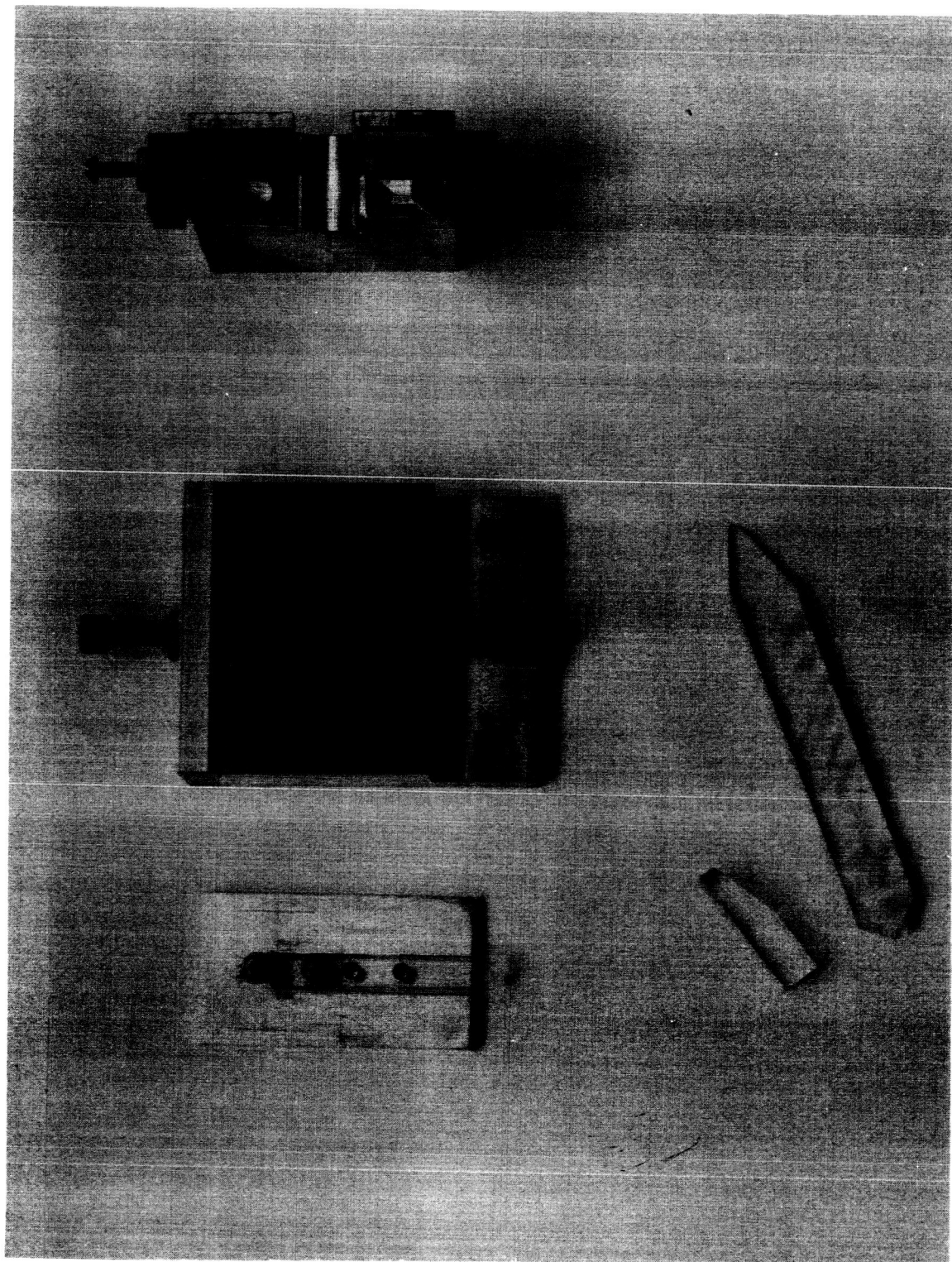


Fig. 6: BRUSH FORMING JKS

VI. INSTRUMENTATION AND APPARATUS

Ring-brush material combinations were evaluated by measurement of electrical noise, contact resistance and drag-torque of experimental capsules operated in various modes. The equipment and apparatus utilized in performing the evaluation are described in the following sections.

A. Drive and Run-In Apparatus

A pneumatically-driven torsion oscillator was constructed for driving the slip-ring capsule in the oscillation mode during measurement of electrical noise. The apparatus was also used for continuous rotation tests and for certain run-in tests. The unit was operated from a nitrogen gas cylinder, and the housing portion was pressurized to provide a dry nitrogen protective atmosphere for the capsule. The torsional system was designed to operate at a frequency of about 10 to 12 cps, and peak to peak deflections up to approximately 8° could be obtained, although most tests were performed at a peak to peak deflection of 0.5° . A pneumatic system was selected primarily to avoid noise and pick-up from a motor or torquer drive.

Basically the torsional oscillator consists of a 3 inch diameter inertial brass cylinder one inch thick and a 1/16 inch steel torsional rod 4-3/8 inches long. The torsion rod is attached to the upper side of the cylinder and the rotor of the experimental capsule to the under side.

Figure 7 is a disassembled view of the torsional drive showing the principal components. The stator of the capsule is placed in a slip-fit well in the frame of the apparatus and secured by tightening a pair of flat plates against two O-rings which spread to hold the stator firmly in position. After

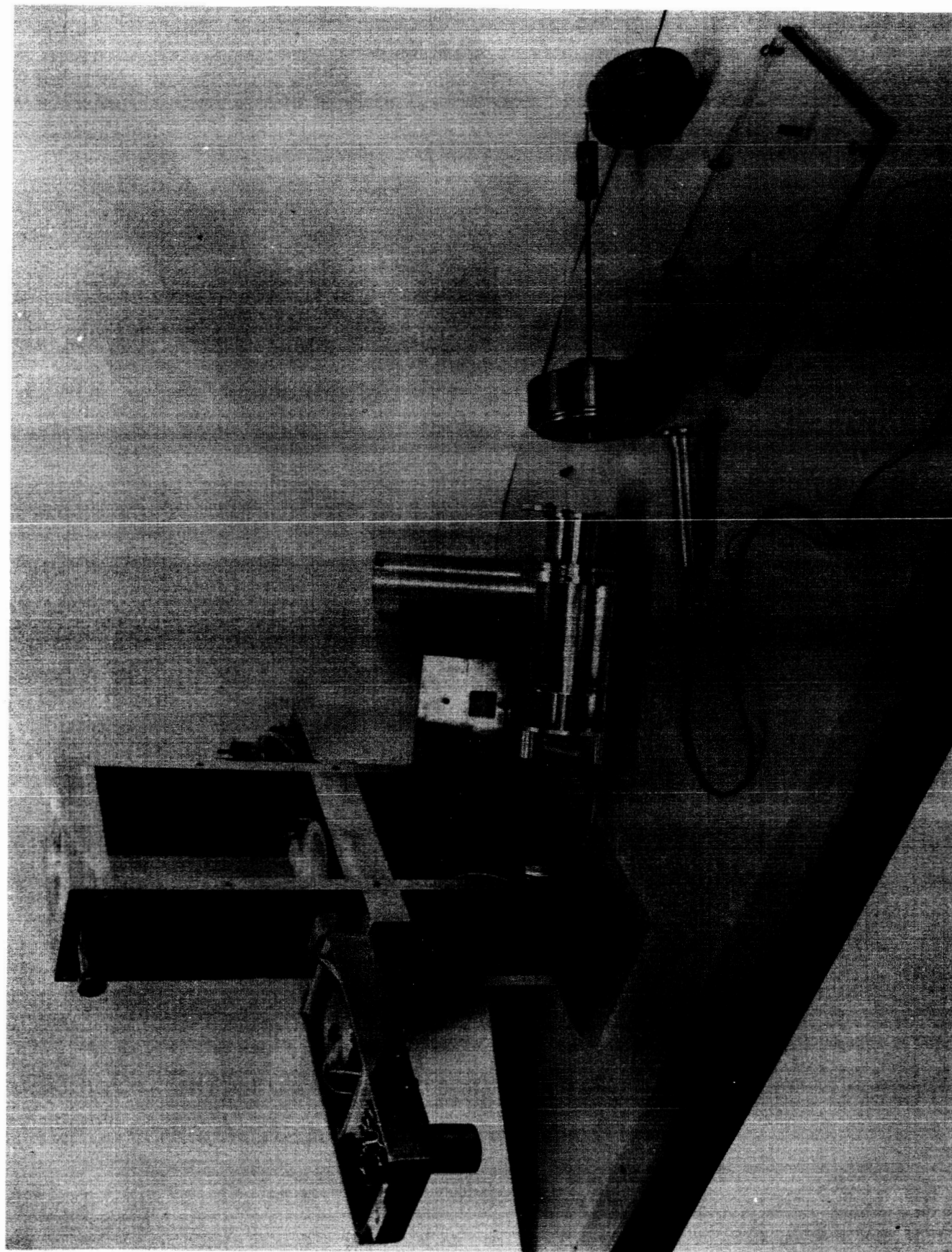


Fig. 7: DISASSEMBLED DRIVE APPARATUS

installation of the stator, the upper "head" of the torsion rod (a 1/2" diameter x 3/4" long brass cylinder silver-soldered to the rod) extends freely above the capsule-cylinder-rod system supported by the stator. One-half of the split cylindrical clamp shown on the right side of Fig. 7 is then adjusted carefully against this uppermost piece and screwed down. Oversize screw-clearance holes permit careful positioning of the clamp. The other half of the split clamp is then screwed to the first half. This method of assembly ensures the absence of undue stresses on the capsule bearings.

The three-inch inertial cylinder has two short arms projecting from it 180° apart. A 1" x 2" iron vane is attached to one arm for monitoring the oscillator frequency and amplitude. The instantaneous angular deflection of the drive is sensed by a permanent magnet type electromagnetic microphone placed about 1/8 inch from the iron vane. The microphone output is amplified by a model 300 Ballantine amplifier, filtered by a 30 cps low-pass filter, and displayed on a CRO. The deflection is calibrated by a Type No. 711-F Starrett dial indicator placed against the projecting arm during adjustment of a given peak to peak angular deflection.

Initially, the torsional system was driven by an expandable rubber tube acting on one projection arm. The system was later modified to permit driving at both projection arms in order to obtain a balanced mechanical couple and avoid introduction of vibrations into the capsule. Figure 8 is a photograph of the driving arrangement that appears on each side of the inertial cylinder. The projection arm presses firmly against the rubber tube by virtue of a pre-set twist of about 10° in the torsion rod at the time of assembly. The inactive tube at the opposite side of the projection arm acts as a bumper or damper and is effective in obtaining sinusoidal deflections.

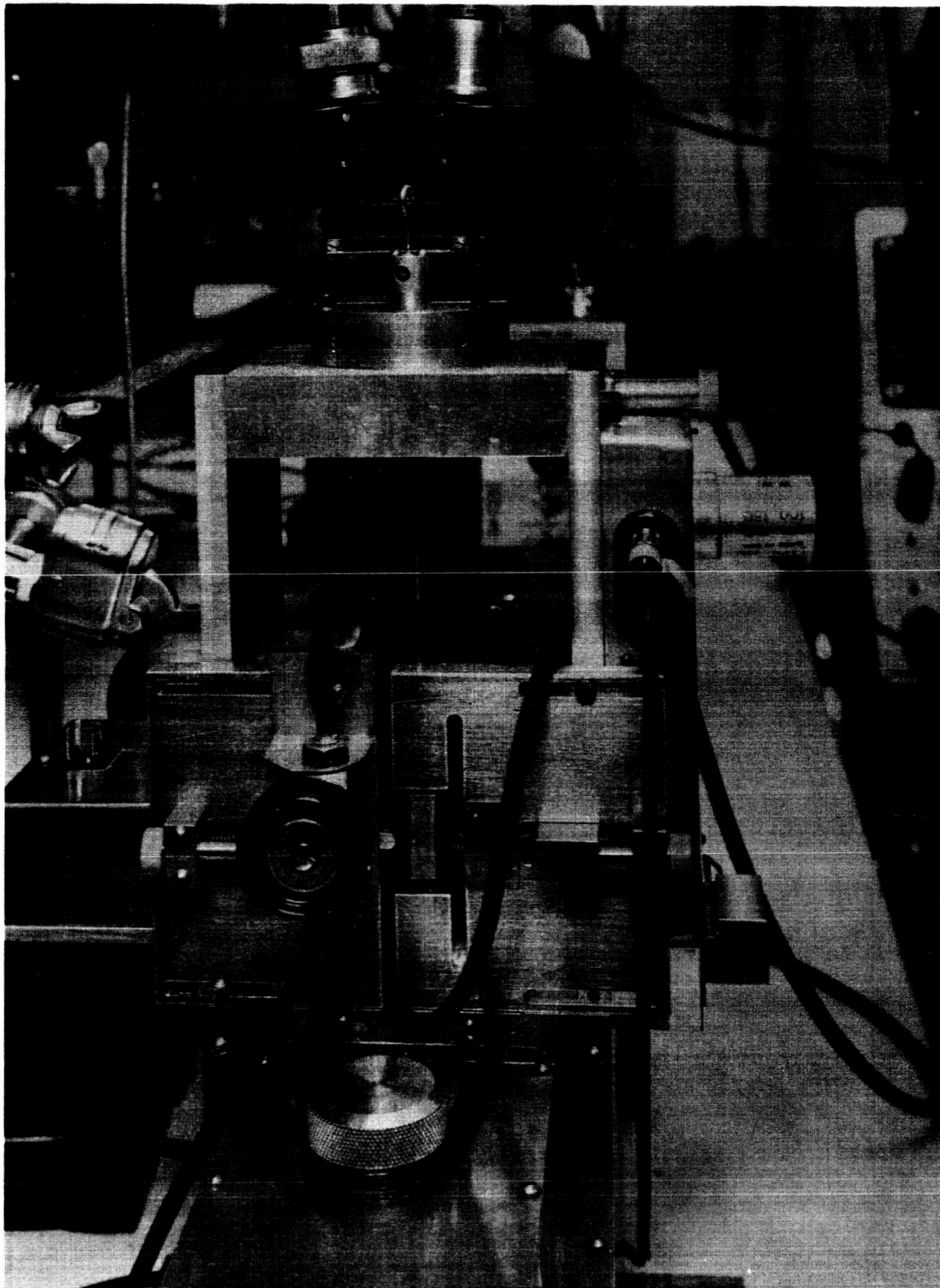


Fig. 8: DRIVING ARRANGEMENT TORSIONAL DRIVE

The active rubber tube is supplied with dry nitrogen at an adjustable pressure of 5 to 10 psi from the supply cylinder. About 5 to 10 cubic feet per hour of gas is used. Beyond the two drive arms the rubber tube terminates at an "oscillating vent" of the same natural frequency as the torsion oscillator.

The oscillating vent consists of a pivoted steel armature that moves synchronously up and down to open and close a 1/16 inch hole near the closed end of the rubber tube. Before the gas is turned on, the weight of the armature effectively closes the 1/16 inch hole in the tube; with the gas on, pressure builds up in the tube and as the rubber stretches, it accomplishes two things: it rotates the capsule-drive and lifts the armature of the venting device. As the latter rises, gas escapes, reducing the driving force of both oscillating systems, causing each to soon begin return excursions. Following subsequent re-closure of the vent, the sequence becomes periodic. To obtain proper resonance between the two systems and good sinusoidal deflection, valves in the gas line must be correctly adjusted. Deflection amplitude is controlled primarily by gas pressure at the inlet side.

The well into which the stator is fitted is arranged to be rotatable by hand or pulley by the provision of a nylon-aluminum 1-5/8 inch slip fit bearing. This permits the angular position of the stator to be altered continuously, intermittently, or to remain stationary as desired.

The stator wires are contained in a split aluminum can which is a part of the rotatable assembly. The split aluminum cylinder is shown in the center of Fig. 7. The wires are wound on slotted aluminum spools just fitting the can and held by machine screws. Attached perpendicularly to the base of the spool is a 10 pin terminal block which permits connection to the brush leads.

For continuous rotation tests, the split cylindrical clamp holding the torsion rod was removed and the capsule rotor-inertial cylinder combination was belt driven by a small synchronous motor. Noise measurements were also made for a free rotation condition in which the rotor was manually spun and allowed to coast. Noise signals were recorded during the coasting process.

The drive apparatus also contained provisions for slowly rotating the stator while the rotor was oscillated by the torsion system. In this mode the stator was belt driven by a speed reducer motor, and by means of a cam operated snap-action switch, the direction of stator rotation was reversed once every complete revolution. The actuator of the reversing switch is visible in Figure 7 in the far port of the drive structure.

In the oscillation tests, it was desirable to identify the points in the deflection cycle with which peak noise spikes were associated. This was accomplished by triggering the oscilloscope from a small external synchronizing switch that was actuated by one of the projection arms of the inertial cylinder. The synchronizing switch was placed in a low voltage battery circuit which delivered a triggering pulse to the scope when the switch was actuated.

Equipment for a 50 hour run-in conditioning process was also fabricated. This equipment consisted of a small enclosure in which the experimental capsule was mounted and in which dry nitrogen gas was circulated to simulate actual operating conditions. The capsule was driven at a constant speed of approximately 350 rpm. This equipment was later modified to permit periodic reversal of the direction of rotation. Electrical noise was monitored during the run-in operation. Synchronizing signals

for viewing noise as a function of rotor position were obtained from a coupling device between the motor and capsule rotor which incorporated a small switching segment.

B. Instrumentation

1. Deflection

For relating the electrical noise and the instantaneous velocity of the sliding contact, measurements were made of the deflection of the rotor as a function of time. In the oscillatory mode, deflection was sensed by the permanent magnet type microphone as described in the preceding section. This system produced a signal which was proportional to the instantaneous velocity of the projection arm having the iron vane.

In the continuous and free rotation noise tests, rotor position and velocity was determined from a photocell arrangement. A circular mask having regularly spaced holes near its edge was attached to the inertial cylinder in a position which interrupted a light beam as the rotor revolved. Pulses from the photocell were amplified and displayed on a scope. Determination of the time between pulses permitted calculation of the incremental velocity of the rotor.

2. Electrical Noise

Electrical noise was measured directly across pairs of brushes by sensing the voltage at the ends of the brush leads when a constant d-c current of 25 milliamperes was passed through the brush circuit. The d-c voltage was supplied by an adjustable Heathkit regulated power supply through an external 500 ohm protective resistor. A 100 μ f, 150 volt electrolytic capacitor was placed across the output of the power supply to minimize

ripple. The voltage drop across two brushes was amplified by a Tektronix Type 122 Low Level Pre-Amplifier and a Keithley Decade Isolation Amplifier and then fed to a Tektronix Type 545A oscilloscope with a Type CA dual trace plug-in unit and a General Radio Type 1521A Graphic Level Recorder. Figure 9 is a block diagram of the noise and deflection instrumentation for evaluation of experimental capsules.

To avoid ground loops, the only grounding of the noise circuit was at the power supply and the Type 122 pre-amplifier. As shown in Fig. 9, the experimental capsule frame was connected to ground only by the shield of the coaxial cable supplying the Type 122 pre-amplifier. The use of the GR Graphic Level Recorder permitted determination of the true rms value of noise while the Tektronix CRO permitted measurement of peak to peak noise from oscillograms of the noise voltage. Figure 10 is a photograph of the general laboratory set-up showing the pneumatic drive and the noise and deflection instrumentation.

3. Drag Torque

The drag torque of the experimental, four brush capsules was measured with a torsional apparatus in which the angular deflection of the torsional element was observed as the capsule was manually rotated. Figure 11 is a photograph of the drag torque apparatus which also shows the microscope used for measuring angular deflection. By means of a micrometer eyepiece, the position of the torsion indicator is observed before and during rotation, and angular deflection is determined from the difference of the two readings. Readings were obtained at numerous stator positions

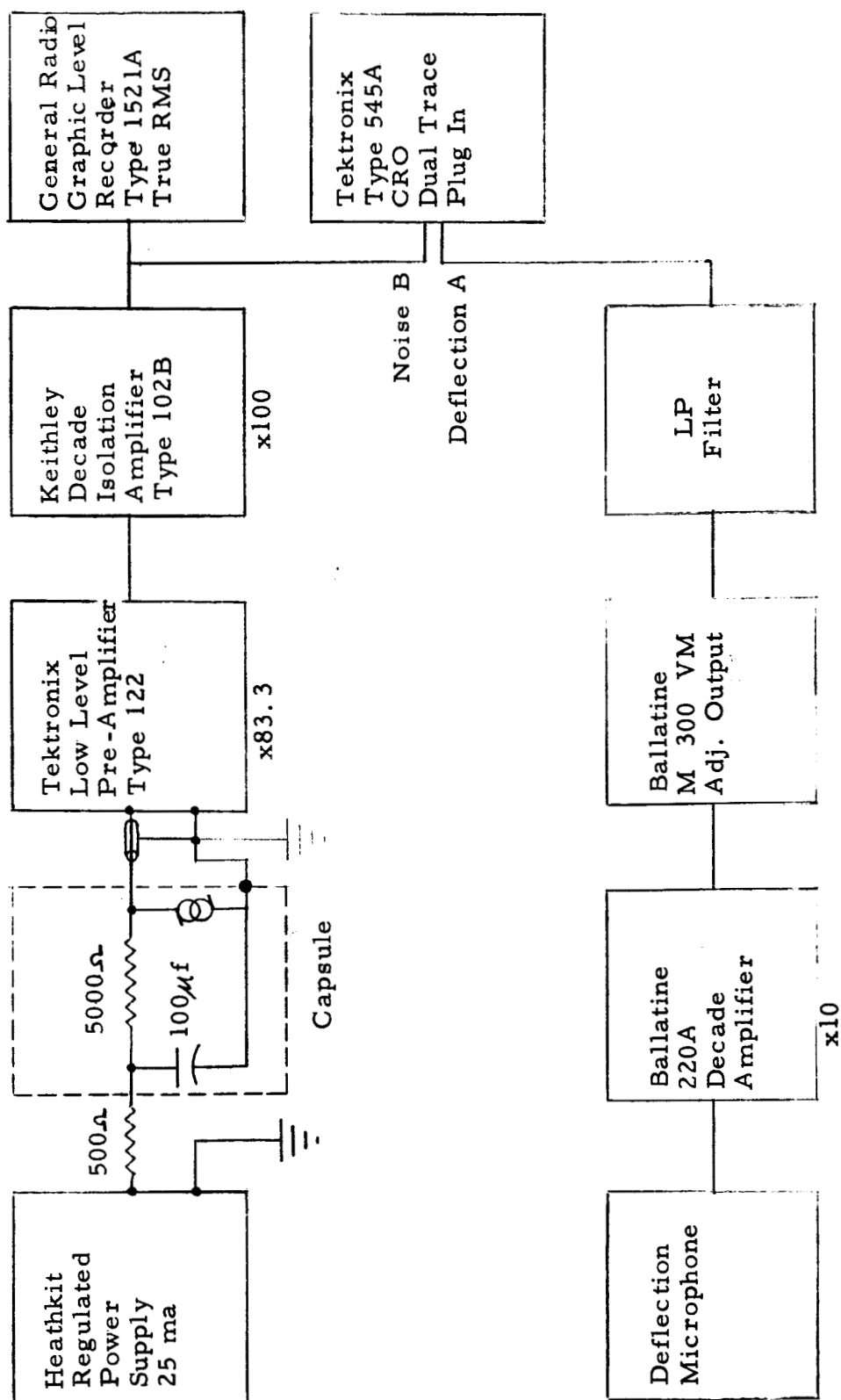


Fig. 9: NOISE AND DEFLECTION INSTRUMENTATION

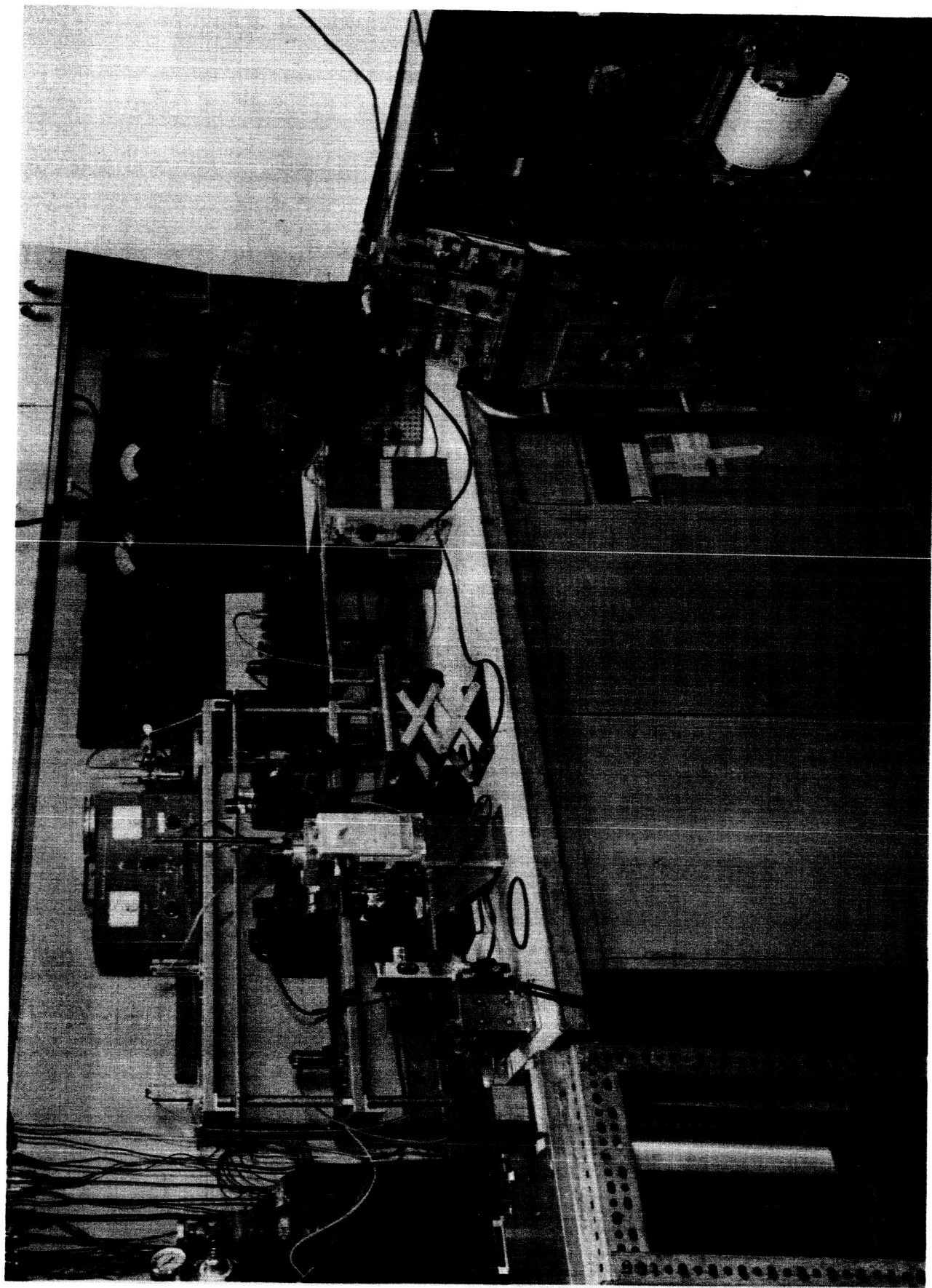


Fig. 10: GENERAL LABORATORY SET-UP

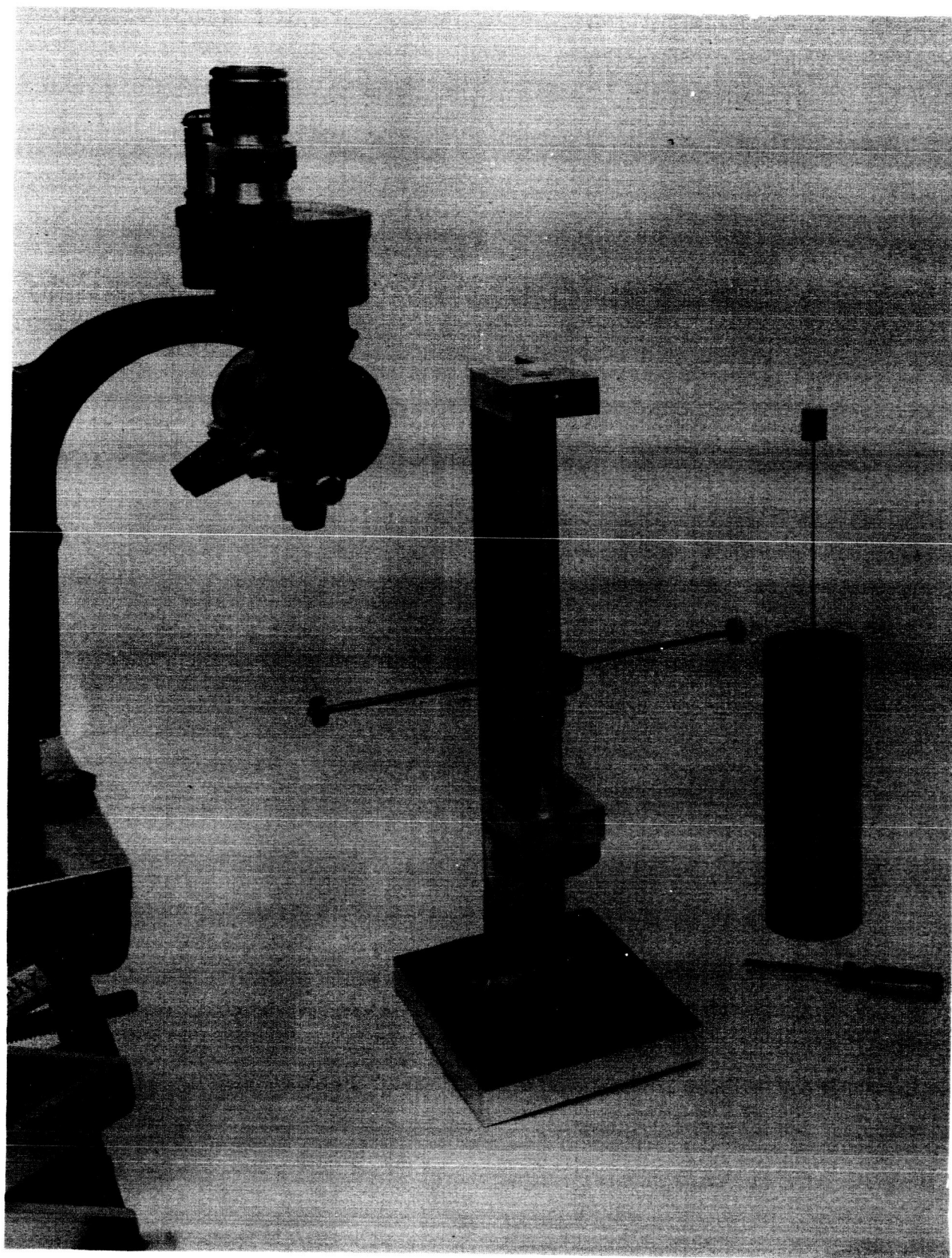


Fig. 11: DRAG TORQUE APPARATUS

for both directions of rotation and then averaged. The inertial cylinder shown at the right of Fig. 11 was used for calibration of the torsional element.

Relative indications of drag torque were also obtained from recordings of the rms deflection during free oscillation tests. The decrement of the rms deflection signal during the attenuation of motion in free oscillation tests is proportional to drag-torque, and comparison of the deflection recordings permitted evaluation of drag-torque on a relative basis.

4. Brush Force

To avoid damage of the brush or ring surface, no adjustments of brush force were made after forming of the Nooteboom brushes. To insure that representative brush forces were obtained in the experimental capsules, a force measurement apparatus was developed which permitted measurement of the force of each individual wiper in an assembled capsule. The apparatus consisted of a glass hook which was accurately positioned by mechanical guides to loop around each brush arm. The mechanical guides prevent damage to the brush during the looping process. The glass hook was then loaded by a calibrated chain until electrical contact between brush and ring was disrupted as determined by an ohmmeter. Figure 12 is a close-up photograph of the brush force apparatus. Determination of the length of chain required to disrupt conduction gives a measure of the brush force. The calibrated scale on the left hand edge of the apparatus gave direct readings of the brush force.

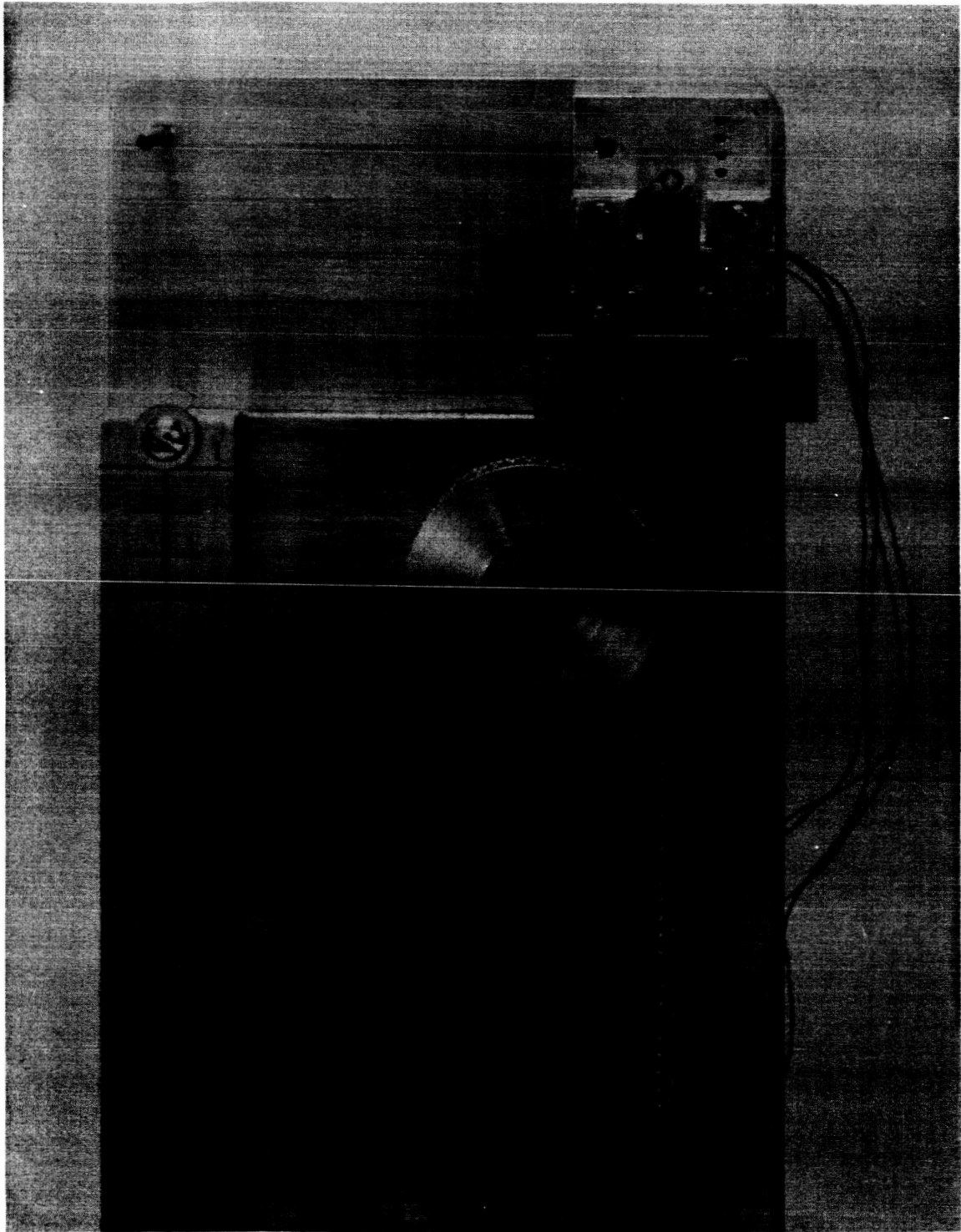


Fig. 12: BRUSH FORCE APPARATUS

VII. LABORATORY EVALUATION - EXPERIMENTAL CAPSULES

A. General Noise Characteristics

Although the primary objective of the laboratory evaluation of experimental capsules was to establish the influence of materials, information was also obtained on other factors contributing to the over-all noise characteristics of miniature slip-ring assemblies. These factors became evident in the course of the experimental work, and it was necessary to continually modify and refine the noise measurement techniques so that the true dependence of materials could be determined.

The electrical noise characteristics of the experimental capsules were determined by sensing the voltage drop across two brush-ring circuits connected in series. If the noise characteristics were completely random in origin, the noise of one brush-ring combination would be $1/\sqrt{2}$ times the measured noise. However, indications were obtained that electrical noise has systematic origins in addition to possible random sources. Oscillograms of noise show that electrical noise has a strong component whose frequency is twice the frequency of the capsule oscillation. Figure 13 is an oscillogram of deflection and noise waveforms which illustrates the double frequency dependency. Also, other oscillograms indicated that electrical noise patterns of all ring brush combinations were in many cases similar for the same angular position of the rotor. This would indicate that noise is influenced by eccentricities of the rotor or by the characteristics of the capsule bearings. Mechanical vibrations were also found to contribute to noise level. Because of the systematic nature of these noise causes, the noise of a single brush-ring circuit is probably closer to $1/2$ the measured noise of two circuits than to the theoretical value for random sources. No attempt was made to establish

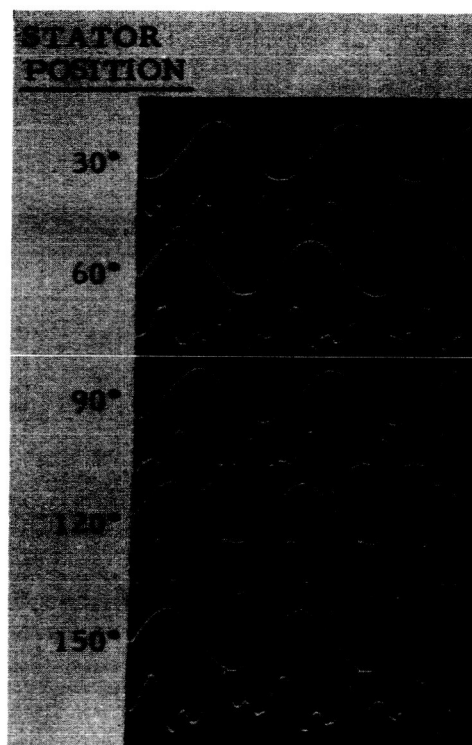


FIGURE 13 - DOUBLE FREQUENCY CHARACTER OF NOISE

the exact relationship since relative comparisons were possible from the noise figures for two circuits.

In the initial pneumatic drive unit, the torsional system was driven only from one projection arm. When a small switch was placed against the other projection arm for the purpose of deriving a synchronizing signal, or when the Starrett micrometer indicator was placed against the arm, it was noted that the character and amplitude of the noise changed. Figure 14 is an oscillogram of deflection and noise traces which shows the loading effect of the micrometer indicator. The "a" and "c" noise traces were obtained with the indicator in its position for angular amplitude measurement. Figure 15 is the GLR recording of the rms value of noise for the corresponding noise traces of Fig. 14. An increase of about 3.5 db in the rms noise was indicated for this particular loading effect. The higher noise resulting from the loading effect was probably due to abnormal side thrust on the capsule bearings caused by the indicator.

The loading effects observed with the initial drive suggested that noise could be induced by mechanical disturbances not originating from contacting surface phenomena. For this reason, the pneumatic drive was modified to permit driving from both projection arms so that a balanced couple was obtained. Elastance matching rubber tube cushions were also added to obtain better deflection waveforms and higher amplitude oscillations. Table 9 presents a comparison of noise measurements before and after the modification for Capsule 1-1B, an early capsule containing soft gold rings. The data demonstrates that noise levels are somewhat dependent upon the method of drive, presumably because of mechanical disturbances that are introduced.

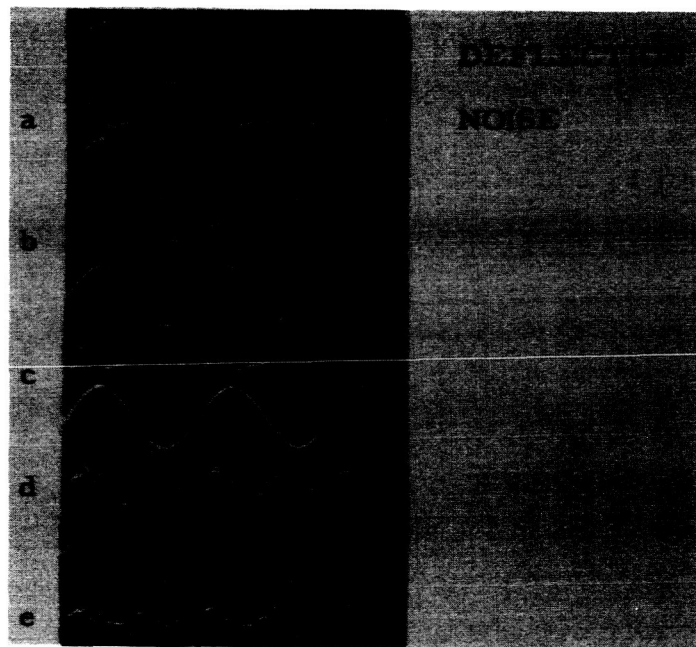


FIGURE 14 - MECHANICAL LOADING EFFECTS

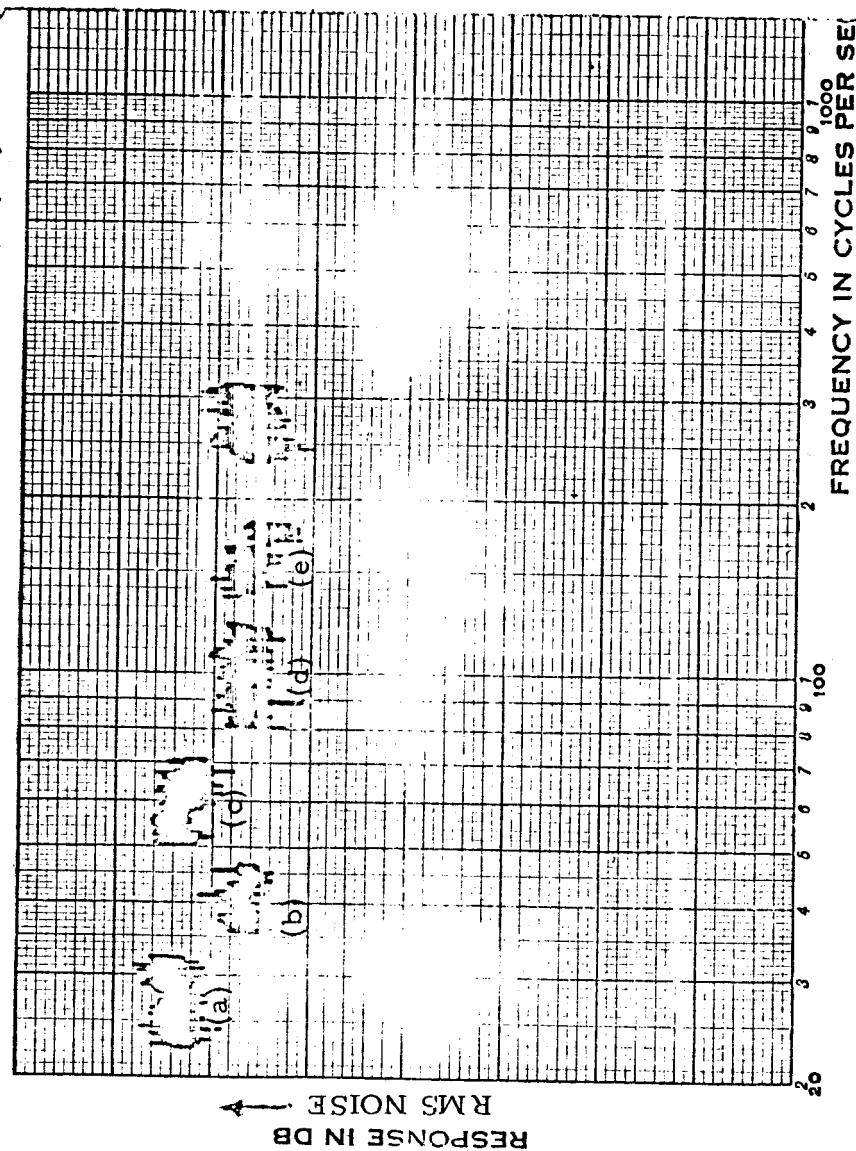


FIGURE 15 - RMS NOISE RECORDINGS CORRESPONDING
TO LOADING EFFECTS OF FIGURE 14

Table 9

NOISE MEASUREMENTS COMPARISON

Capsule 1-1B

Average RMS Noise at Brush Current of 25 ma

<u>Before Drive Modification</u>		<u>After Drive Modification</u>	
<u>Peak to Peak Deflection</u>	<u>Electrical Noise - μv</u>	<u>Peak to Peak Deflection</u>	<u>Electrical Noise - μv</u>
0.0°	0.50	0.18°	0.84
0.2°	0.80	0.27°	1.58
0.3°	2.8	0.41°	2.51
0.4°	4.2	0.74°	2.98
0.5°	4.5	1.0°	2.66
0.6°	4.5	1.6°	2.98
0.7°	4.7	3.3°	2.66
		6.0°	2.98
		11.8°	3.16

Since the modified drive permitted peak to peak angular deflections up to approximately 12° at a constant frequency of 11 cps, a series of measurements were made to establish the dependence of noise on angular deflection. The noise-angular deflection relationship really infers a dependence of noise on the velocity of the sliding contact. Figure 16 shows the general relationship that was obtained for all experimental capsules. At very small angular deflections below about 0.4° ptp, noise exhibits an almost linear relationship with deflection (or velocity). Above a fairly specific deflection, noise level is generally uniform and shows almost no dependence on further increases of peak to peak deflection angles. Although the specific data shown in Fig. 16 refers to Capsules 1-1B and 2-10 after 50 hours of run-in, the same general threshold effect was observed with all materials, both before and after run-in.

It was postulated that the transition between the linear region and the uniform regions occurs at deflections where rolling contact stops and sliding contact begins. Because of the flexible nature of the Nootboom brush, small angular deflections may not cause sliding action between the brush and ring. In such cases, a specific contact point between the brush and ring may roll with the ring if the deflection is within the motion that is permissible by flexure of the Nootboom brush. Such action has been described as a rolling contact. Table 10 presents a tabulation of the noise transition points of Capsule 2-10 for seven different angular positions of the stator. As indicated, the average drop-off point was about 0.4° for the Neyoro 28A brush - hard gold "A" overlay ring system. A theoretical analysis of the radial motion that is possible with the Nootboom brush of proper dimensions indicated that deflections of 0.35° ptp were possible before sliding action between brush and ring took place.

IIT RESEARCH INSTITUTE

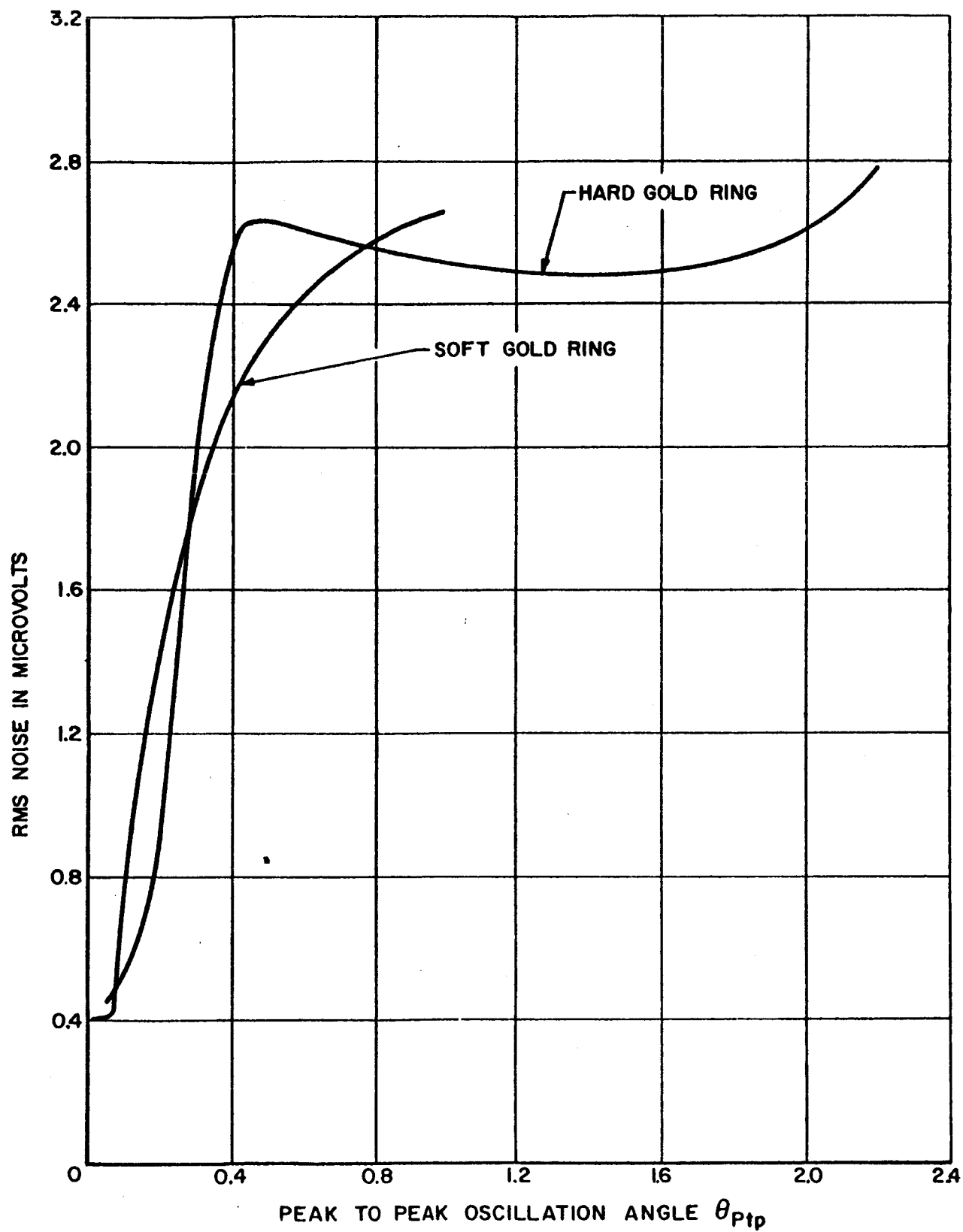


FIG. 16: NOISE SIGNATURES
IIT RESEARCH INSTITUTE

Table 10
NOISE TRANSITION POINTS
 Capsule 2-10

Stator Position	Point of N_{2RMS} Drop-Off O_{ntp}
5°	0.44°
65°	0.56°
125°	0.40°
185°	0.28°
245°	0.28°
305°	0.44°
335°	0.56°
Average	0.42°

At this stage in the laboratory evaluation, the question arose as to whether mechanical disturbances were completely eliminated, even in the balanced drive apparatus. To minimize the possibility of mechanical disturbances influencing the noise measurements, a completely passive method was adopted for measurement of noise. In this method, the driving elements of the torsional system were removed, and the projection arms of the inertial cylinder were manually deflected against a fixed stop. The inertial cylinder was then released and the system was allowed to oscillate freely until its motion attenuated to zero. During the oscillation interval, noise and deflection signals were recorded simultaneously. Figure 17 is a GLR recording of the rms deflection and noise signals during a free oscillation test for one stator position of Capsule 2-10, a capsule containing rings of soft gold with a hard gold "A" overlay. The noise trace of Fig. 17 exhibits the typical threshold effect observed with all capsules.

Although the free oscillation method of noise measurement minimizes the mechanical disturbances introduced by driving elements, it only permits evaluation of one position of the ring surface, and hence it does not portray the general performance of the ring-brush system. To determine the amount of variation that exists in any one brush-ring combination, free oscillation tests were performed at seven different positions of the stator for capsules 1-1B and 2-10. Tables 11 and 12 summarize the noise measurement data and give an indication of the variation that occurs in typical experimental capsules. The data for Capsule 2-10 was used to prepare a composite chart which illustrates the average deflection and noise performance during free oscillation tests. This composite is shown in Fig. 18. It further demonstrates the threshold noise effect.

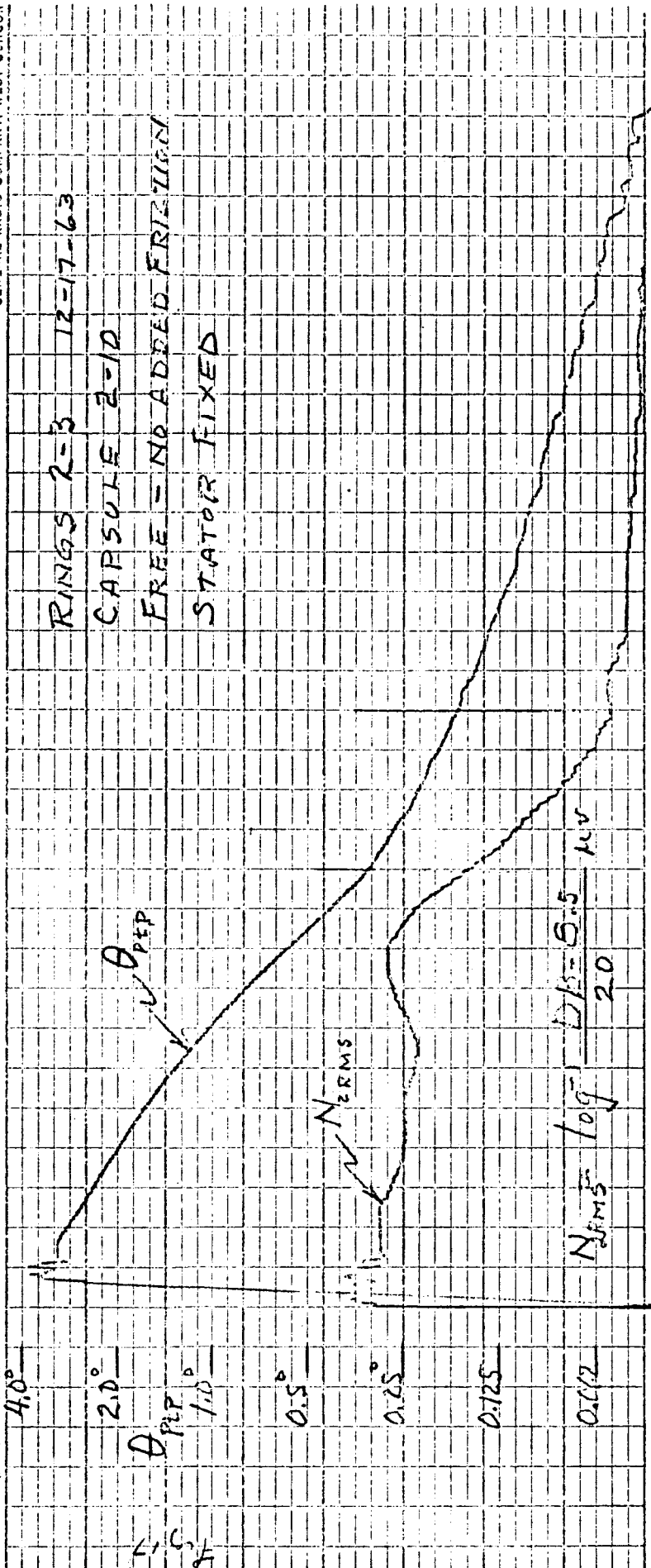


FIGURE 17 - RMS DEFLECTION AND NOISE DURING

FREE-OSCILLATION TEST

Table 11
Noise Signature Data
 Capsule 1-1B (Soft Gold)

θ° ptp	$N_{2rms}(db)$ at							$N_{2rms}(db)$ Average	N_{2rms} Micro-volts
	0°	60°	90°	180°	240°	300°	330°		
0.912°	15.2	18.3	16.0	18.5	16.0	15.8	18.8	16.9	2.63
0.610°	15.0	18.3	15.2	16.5	15.0	15.2	19.0	16.3	2.45
0.473°	14.0	18.3	15.0	16.0	13.5	14.5	18.0	15.6	2.26
0.343°	14.8	17.3	16.0	14.8	11.0	12.5	14.5	14.4	1.97
0.248°	12.5	15.8	15.0	14.4	8.3	10.9	11.8	12.7	1.62
0.186°	9.8	15.5	12.5	13.2	7.1	8.5	8.8	10.8	1.30
0.119°	4.2	9.9	6.5	7.0	6.0	4.0	2.4	5.7	0.72
0.086°	2.3	11.1	3.3	2.3	3.0	2.4	1.2	3.7	0.58
0.062°	1.1	3.0	1.2	0.0	0.4	1.7	0.6	1.1	0.43
0.043°	0.7	1.5	1.0	0.0	0.0	0.8	0.4	0.62	0.40

Table 12

Noise Signature DataCapsule 2-10 (Soft Gold-100 μ -in Hard "A" Overlay)

Θ° ptp	N_{2rms} (db) at							N_{2rms} Ave. (db)	N_{2rms} Micro Volts
	5°	65°	125°	185°	245°	305°	335°		
2.16°	18.0	16.0	16.2	17.0	16.0	18.4	18.9	17.2	2.72
1.48°	18.0	17.0	15.0	16.5	15.3	18.0	15.2	16.4	2.48
0.94°	19.0	17.7	15.0	13.2	15.8	17.0	19.3	16.6	2.54
0.56°	18.3	16.0	17.4	14.6	17.1	17.7	19.0	17.2	2.72
0.32°	16.0	11.2	15.8	13.9	16.1	15.5	15.0	14.8	2.07
0.21°	7.2	6.0	9.8	11.0	11.0	10.0	8.5	9.1	1.07
0.16°	4.0	3.8	5.1	5.0	6.0	7.0	6.0	5.3	0.69
0.13°	1.7	2.5	2.5	3.0	5.7	4.7	7.3	3.9	0.59
0.086°	1.5	2.0	2.0	2.0	3.5	3.8	6.0	3.0	0.53
0.060°	0.0	1.1	2.0	1.3	0.7	2.5	5.0	1.8	0.46
0.040°	-1.0	2.0	2.0	1.1	0.4	0.0	1.0	0.8	0.41

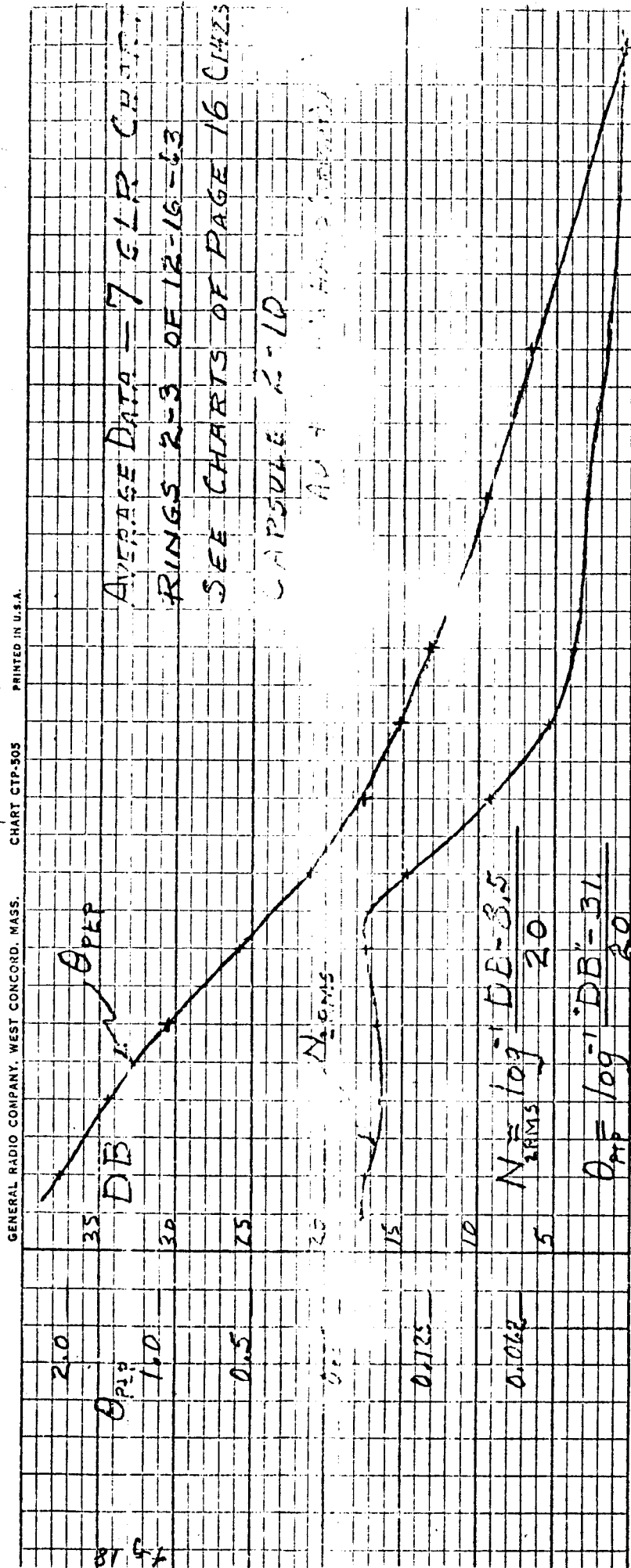


FIGURE 18 - COMPOSITE OF FREE-OSCILLATION TESTS
 AT SEVEN STATOR POSITIONS - CAPSULE 2-10

A noise measurement technique that was found to be extremely useful and effective in overcoming many of the inherent limitations of the other methods was the free rotation test. In this method, the torsional element of the drive was decoupled, allowing the inertial cylinder-rotor combination to rotate freely on its own bearings. The rotor combination was then given an initial spin and the system was allowed to coast. During the coasting interval, GLR recordings were made of rms noise. This method of noise measurement eliminates mechanical disturbances of driving elements since it relies entirely on inertial effects during the coasting process, and it has the further advantage that the condition of all points on the ring surface can be evaluated.

A light source photocell arrangement was incorporated into the apparatus to obtain synchronizing signals and to permit measurement of the rotational velocity during the free-rotation noise tests. Figure 19 is a GLR recording of the rms noise of Capsule 2-17 during the coasting period of a free-rotation test. The noise signal shows that noise level remains essentially constant until velocity has decreased to some threshold value. At velocities below this value, the noise decreases almost linearly with further attenuation of motion. This result supports the results of the driven and free oscillation noise measurements and demonstrates the threshold effect of velocity on noise.

Figure 20 shows three oscillograms of noise during a free-rotation test of Capsule 2-17. In these oscillograms, the alternate traces are the photocell outputs, and the region between two photocell pulses corresponds exactly to one complete revolution of the rotor. The last two noise traces of the third oscillogram show the noise character just before rotation has stopped. All oscillograms were made with a sweep

IIT RESEARCH INSTITUTE

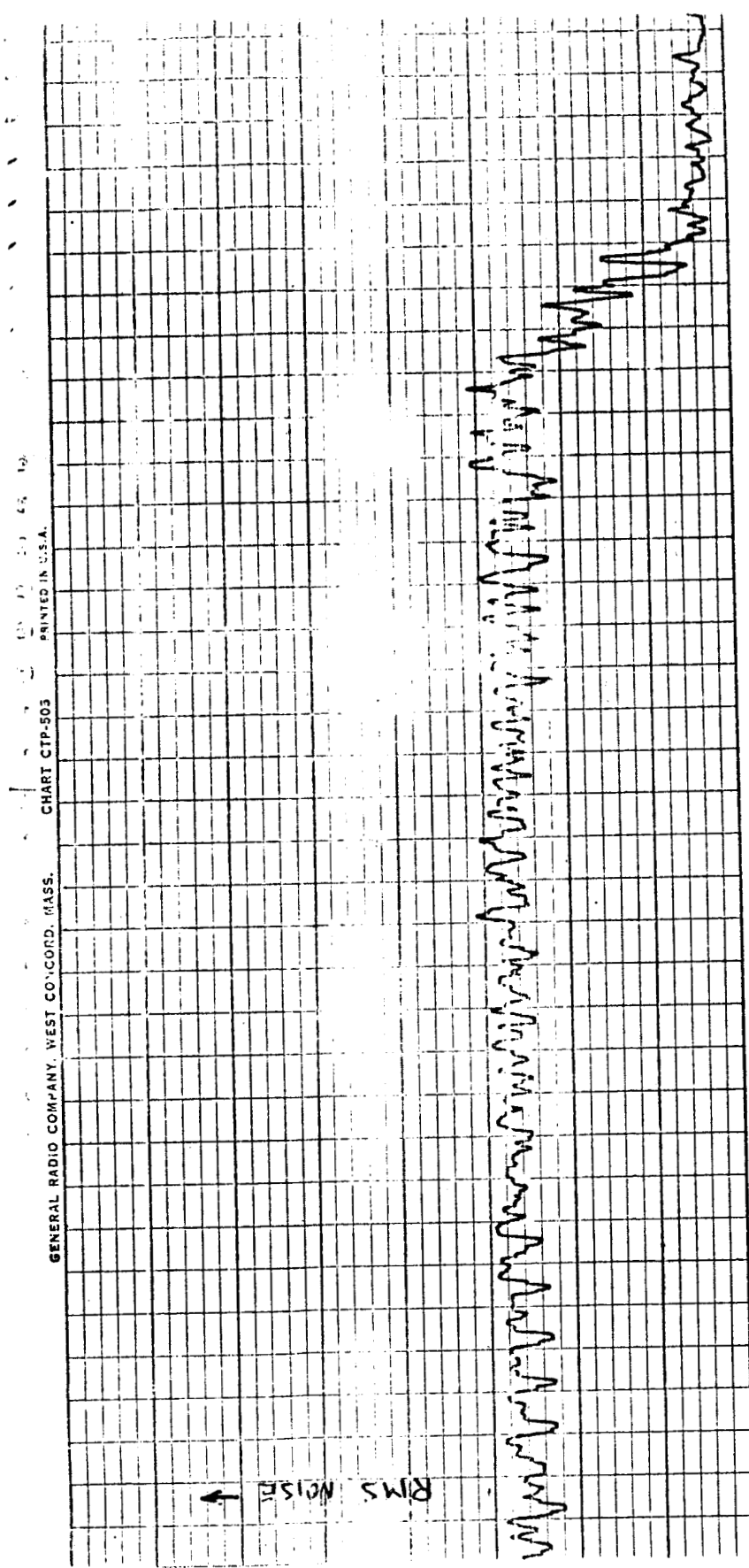


FIGURE 19 - RMS NOISE DURING FREE-ROTATION TEST

CAPSULE 2-17

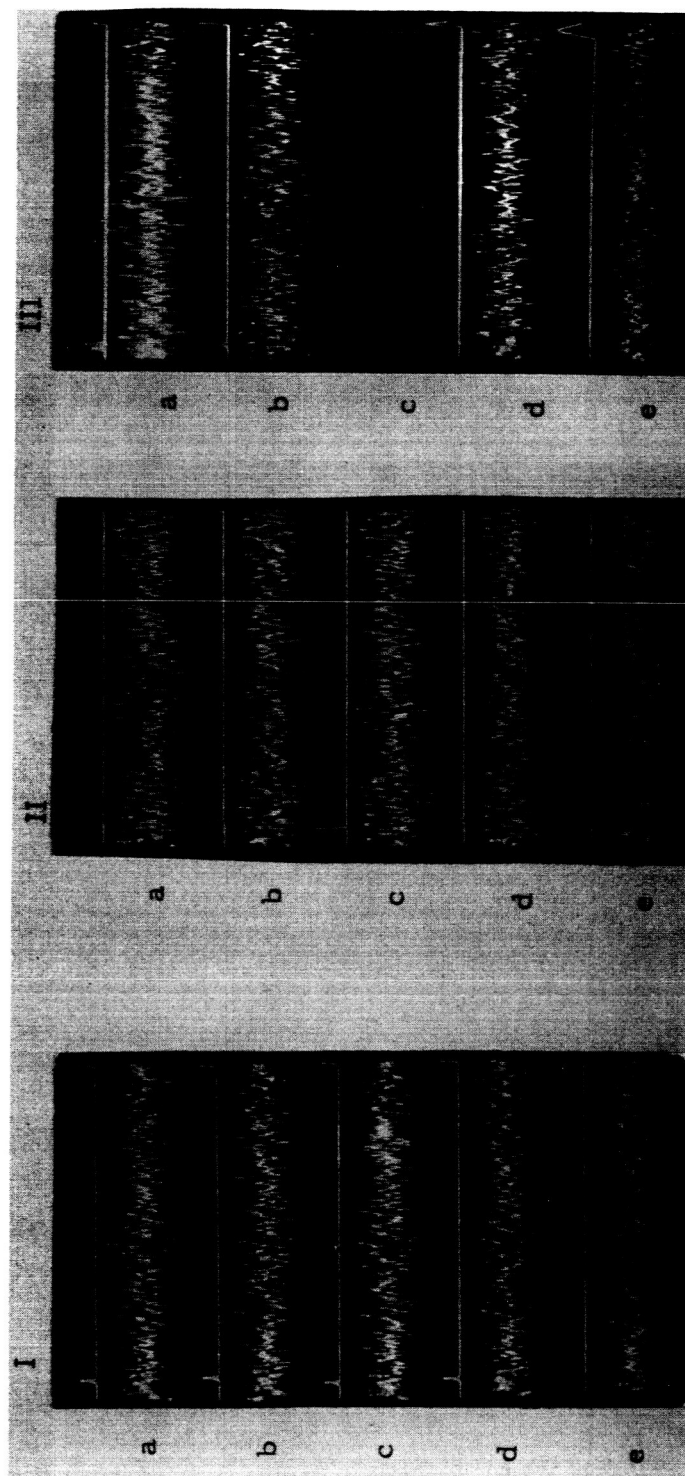


FIGURE 20 - NOISE OSCILLOGRAMS - FREE ROTATION TESTS

CAPSULE 2-17

speed of 0.05 sec/cm. These oscillograms are presented to demonstrate the tendency for the noise patterns to repeat with regard to rotor location, a characteristic which is clearly evident in the first two oscillograms of Figure 20. This result implies that noise spikes are related to the surface condition at specific locations along the ring.

The free rotation tests also gave one other significant result. At the end of each free rotation test, it was found that the rotor oscillated slightly just before motion stopped. This effect is believed to be related to the rolling action of the brushes. When the rotation approaches zero velocity, the sliding contact stops and the brushes tend to deflect back toward their equilibrium positions. Because of friction between the brush and ring, this deflection causes the rotor to oscillate until the neutral positions of the brushes are achieved. The frequency of the end oscillation was found to be about 2.5 cps with a corresponding amplitude of about 0.37° ptp. As indicated in Figure 20X, no noise (above background) was discernible during the end oscillation period as would be expected if no sliding contact occurs.

A series of additional measurements were made to establish the dependence of noise on brush current. A capsule having soft gold rings was oscillated at 10 cps with a deflection of 1.8° ptp. Rms and peak to peak noise were measured for brush currents of 5, 10, 15, 20 and 25 ma. Plots of noise versus brush current indicated an almost perfect linear relationship for both the rms and peak to peak measurements. A series of measurements was also performed to determine the frequency spectrum of the noise. The upper frequency cut-off of the Tektronix 122 low-level pre-amplifier was adjusted to 50 cps, 250 cps, 1kc, 10 kc, and 40 kc, and noise measurements for each position were obtained. The data indicated

IIT RESEARCH INSTITUTE



END OSCILLATION

END OSC. NOISE

PHOTOCELL OFF

TYPICAL NOISE

END OSCILLATION

END OSC. NOISE

PHOTOCELL OFF

BACKGROUND NOISE

END OSCILLATION

END OSC. NOISE

SWEEP - 0.1 sec/cm

FIGURE 20 X END OSCILLATION EFFECTS

that the rms capsule noise contains less than 1.5 db that is attributed to components of greater than 50 cps. The capsule noise therefore consists primarily of components in the 0-50 cps band. All other noise measurements discussed in this report were made with the upper frequency cut-off of the pre-amplifier set at 50 cps.

B. Run-In Effects

Laboratory experiments were also performed to establish the effects of various run-in procedures. The run-in procedures evaluated were continuous rotation, and continuous rotation with frequent reversal of rotation.

1. Continuous Rotation

Continuous rotation run-in was performed in a dry nitrogen atmosphere at a velocity of approximately 360 rpm. A synchronizing attachment permitted monitoring of the noise with respect to the angular position of the rotor. A 100 hour run - in test was performed with Capsule 2-10, and it was found that the noise pattern exhibited good repeatability with respect to angular position. Figure 21 is an oscillogram of noise during the early stages of run-in which demonstrates the repeatability and shows peak to peak noise of approximately 75 microvolts. After approximately 30 hours of run-in, unusually high noise levels were recorded with peak to peak spikes approaching 500 to 600 microvolts. Oscillograms of the noise pattern during the 100 hour period indicated that large voltage spikes were obtained with almost perfect repeatability. This would indicate the debris deposits or imperfections in the ring surfaces caused bouncing of the brush wiper at specific positions along the surface.



23 MINUTES

30 MINUTES

45 MINUTES

60 MINUTES

75 MINUTES

FIGURE 21
NOISE OSCILLOGRAMS DURING 100 HOUR RUN-IN

CAPSULE 2-10

After 100 hours of run-in, the capsule was disassembled and the ring and brush surfaces were inspected. Although a dark deposit was detected at certain points along the bottoms of the ring grooves, almost no permanent damage to the ring and brush surfaces was observed. It was postulated that the high noise levels obtained during run-in were due to the dark deposits which caused lifting of the brush wiper. It was also decided that in the next run-in test, frequent reversals of rotation would be utilized for displacing any accumulation of wear or contaminant deposits.

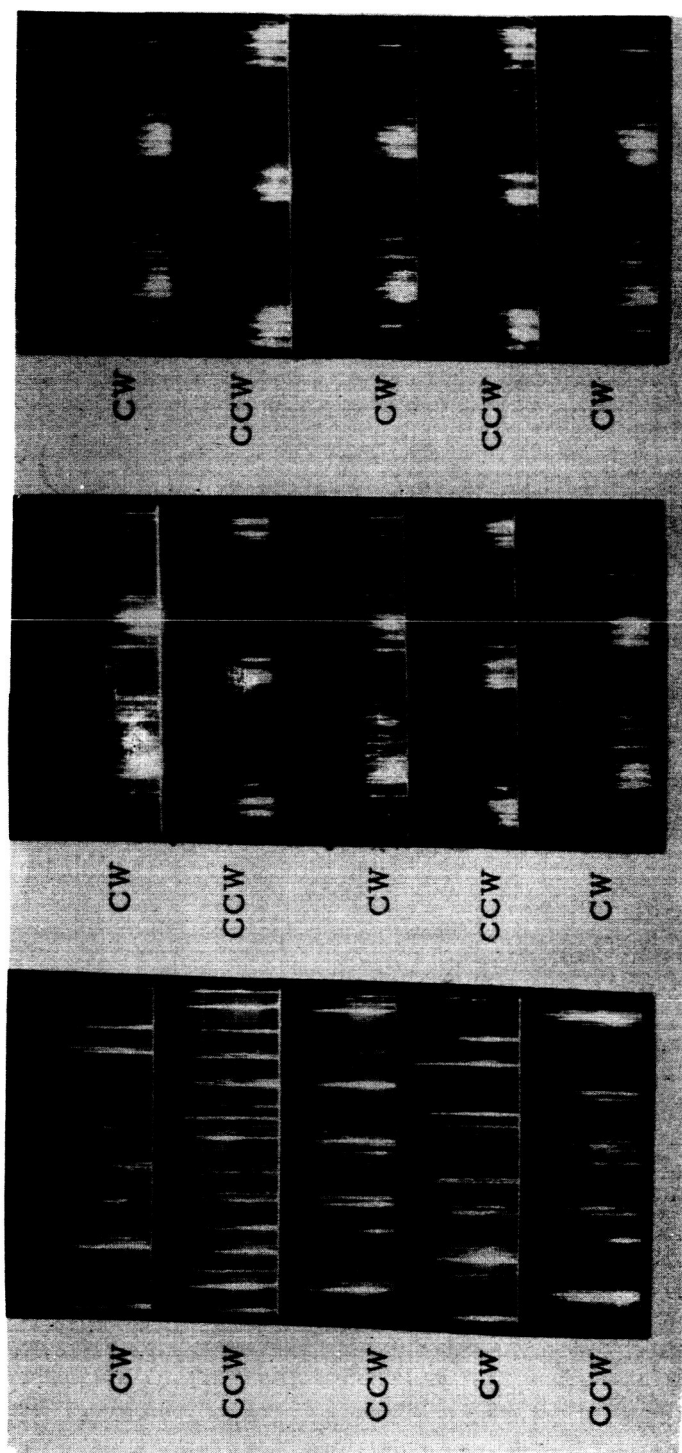
After run-in inspection, Capsule 2-10 was cleaned, rinsed with distilled water, and reassembled. Free oscillation noise measurements were made at seven positions of the stator to establish the over-all effects of run-in. Table 13 is a comparison of rms noise measurements of Capsule 2-10 before and after the 100 hour run-in. As indicated, the threshold noise level was reduced from 6.4 to 2.7 microvolts, a result which is considered to be significant even though both figures were low by accepted standards. Oscillograms of noise after run-in indicated that fewer large noise spikes were obtained, apparently because of the polishing action of run-in.

2. Continuous Rotation with Frequent Reversals

The run-in apparatus was further modified to permit reversal of rotation at 30 second intervals during run-in. Capsule 2-17, a capsule containing rings of soft gold with a hard gold "B" overlay was placed in the modified apparatus and a run-in test was initiated. After approximately 26 hours of run-in, the character of the noise pattern changed from reasonably normal to a series of relatively high-voltage pulses. Figure 22 shows three oscillograms obtained by connecting the capsule output lead directly to the d-c input of the 545A oscilloscope, a procedure that was

Table 13
EFFECTS OF CONTINUOUS ROTATION RUN-IN
 Capsule 2-10

<u>Before Run-In</u>		<u>After Run-In</u>	
<u>Deflection</u>	<u>RMS Noise</u>	<u>Deflection</u>	<u>RMS Noise</u>
0.25° ptp	1.00 μ v	0.13° ptp	0.59 μ v
0.3	1.5	0.16	0.69
0.4	3.8	0.21	1.07
0.5	4.7	0.32	2.1
0.6	6.7	0.56	2.7
0.7	6.3	0.94	2.5
		1.48	2.5
		2.16	2.7



ALL 20 EXPOSURES ALL 10 EXPOSURES ALL 10 EXPOSURES

FIGURE 22 NOISE OSCILLOGRAMS - CAPSULE 2-17 RUN-IN

necessary to overcome loading of the pre-amplifiers. The pulses indicated by these oscillograms were of the order of 1 volt or higher. Since the noise pulses were of short duration, multiple exposures were made by leaving the camera shutter open for 10 or 20 sweeps. When this was done, it was found that for a given direction of rotor rotation the noise pulses were reinforcing or concentrated at specific locations along the ring. This indicated that the noise pulses were associated with ring condition at specific positions along the ring.

Because of the unusually high noise level, the run-in test of Capsule 2-17 was discontinued after 54-3/4 hours of operation. The capsule was disassembled and photomicrographs of the rings and brushes were made. These photomicrographs are shown in Figs. 23, 24, and 25. As indicated, large quantities of wear and/or contaminant deposits were found in the ring grooves and also along the edges of each groove. However, cleaning of the grooves and brushes revealed that little mechanical damage resulted to the ring and brush surfaces.

Free-oscillation tests were performed on Capsule 2-17 after cleaning and reassembly. Figure 26 is a GLR recording showing the rms deflection and noise signals at one position of the stator. The threshold noise level was 1.5 microvolts after run-in as compared to 5.9 microvolts before run-in. This result again demonstrates the useful effect of run-in and a subsequent cleaning operation.

Additional run-in tests were made in the pneumatic drive apparatus by decoupling the torsional element and driving the rotor at 200 rpm with a small 25 volt hysteresis motor. After a period of approximately 30 hours, extremely high noise levels were observed, and over-all results similiar to those of the other run-in procedures were obtained.

IIT RESEARCH INSTITUTE

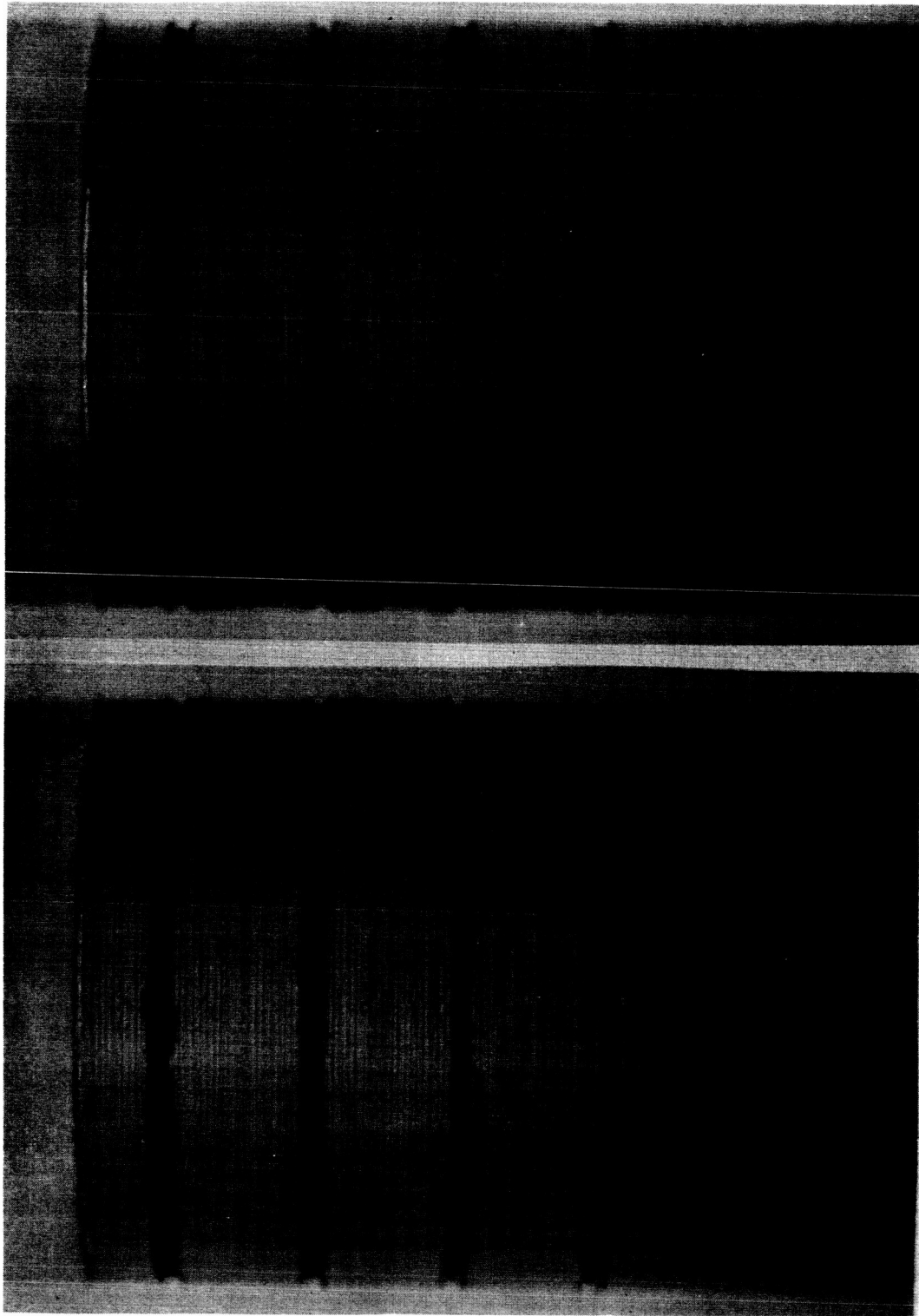


FIGURE 23 - PHOTOMICROGRAPHS
CAPSULE 2-17 AFTER RUN-IN

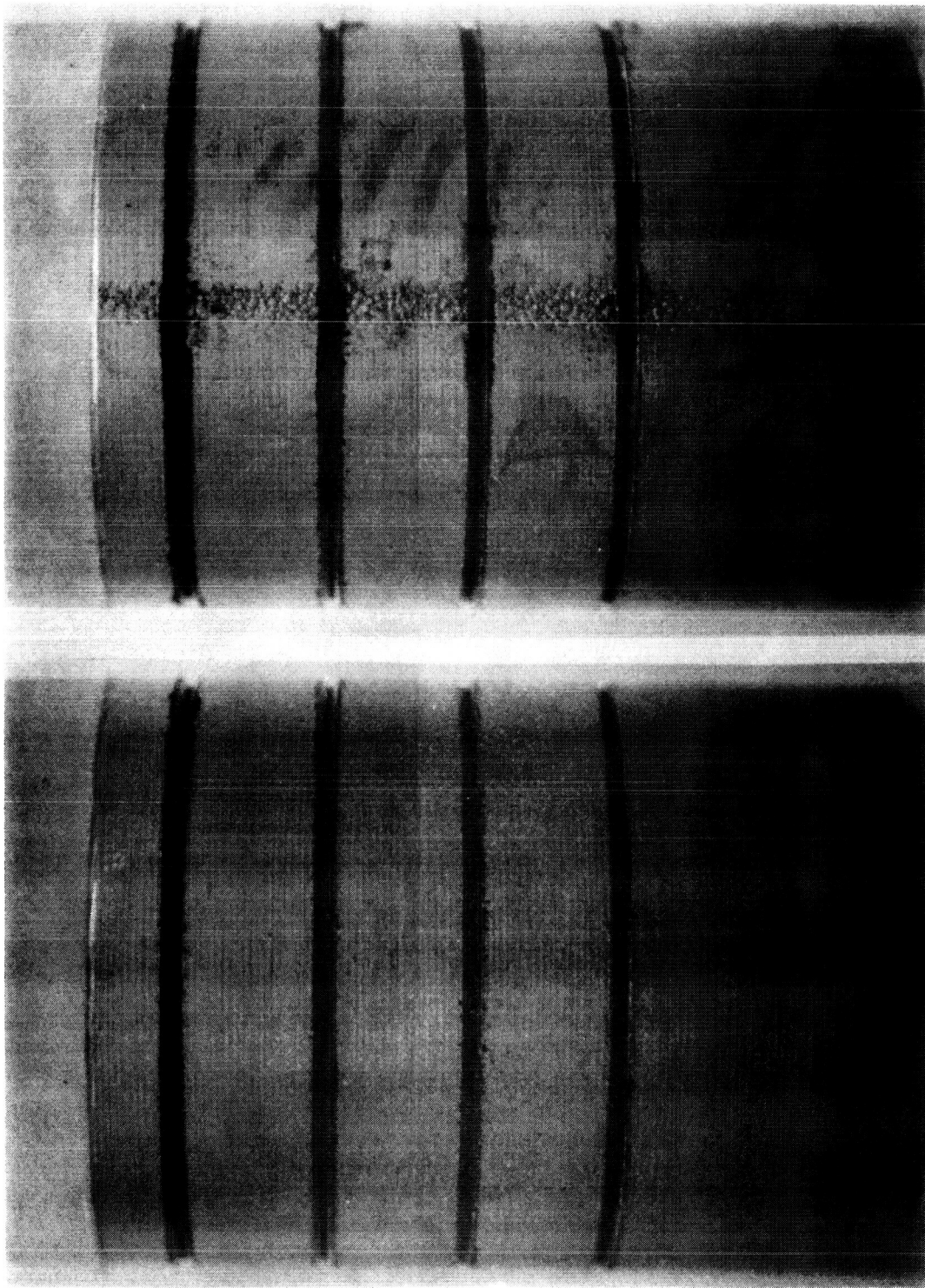


FIGURE 24 - PHOTOMICROGRAPHS
CAPSULE 2-17 AFTER RUN-IN

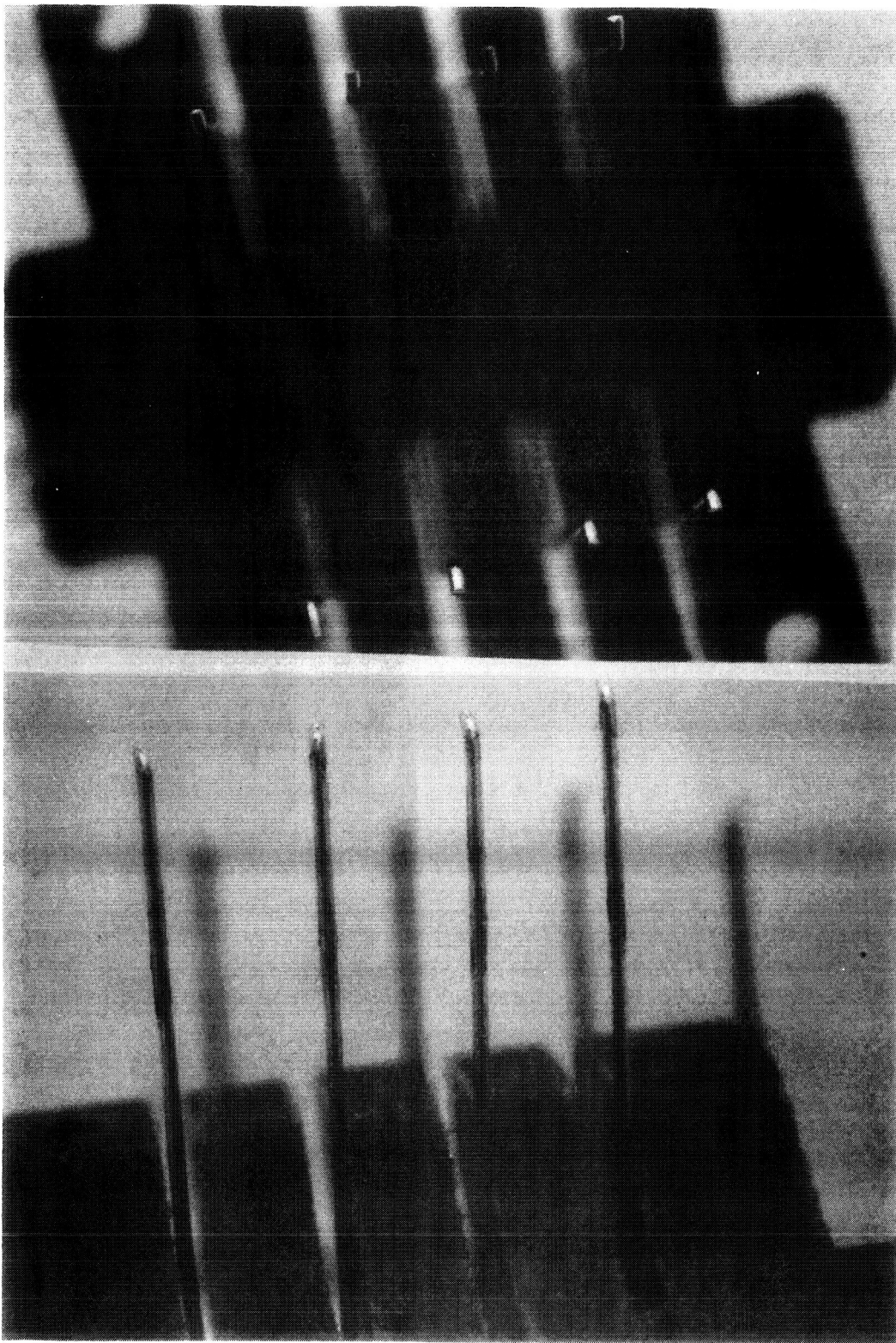


FIGURE 25 - PHOTOMICROGRAPHS
CAPSULE 2-17 AFTER RUN-IN

The general effect of all run-in procedures was the reduction of rms and peak to peak noise after cleaning and reassembly even though extremely high noise levels were recorded during the run-in. This indicated that the high noise levels were associated with the wear and/or contaminant deposits that were subsequently removed in the cleaning operation.

C. Capsule Summaries

Table 14 summarizes the general results that were obtained by laboratory evaluation of experimental capsules. As indicated, the noise levels observed with the soft gold and the two hard gold systems were extremely low in view of the accepted noise standard of 10 microvolts per milliampere of brush current. These results are believed to be attributable to the passive drive methods that were employed in the noise measurements.

Table 14 further indicates that rhodium plated rings are not suited for low noise slip ring assemblies. Evaluation of the rhodium system beyond the initial noise measurements was not carried out because of the relatively high initial noise levels that were recorded.

Capsule 1-36 was comprised of the ring cylinder that was plated from the soft gold bath containing the suspension of fine graphite particles. Preliminary evaluation of Capsule 1-36 indicated that the capsule had an unusually high drag-torque. Nevertheless, the capsule was mounted in the drive apparatus and run-in was initiated. Although the initial noise level was quite low, as shown in Table 14, the capsule soon developed such high drag torque that the hysteresis motor could not bring the system up to the synchronous speed. The test was therefore stopped, and the

Table 14

CAPSULE SUMMARIES

Capsule	Ring Material	Average Brush Force Grams	Average Drag Torque Gram-Cm	Average Threshold Noise at 25ma-2 Rings				Average Resistance 2 Ring Circuit ohms
				Before Run-In		After Run-In		
				RMS μv	Peak to Peak μv	RMS μv	Peak to Peak μv	
1-1B	Soft Gold	2.59	5.12	4.7	34.8	2.6	21.6	0.546
2-10	Hard Gold "A"	2.74	5.35	6.4	32.4	2.7	24.0	0.543
2-17	Hard Gold "B"	2.60	4.55	5.9	31.3	1.5	19.4	0.537
2-21	Rhodium	2.57	----	26.6	44.5	----	----	----
1-36	Soft Gold Graphite	2.60	13.8	3.0	31.8	----	----	----
1-28	Soft Gold	3.07	7.26	2.9	24.0	----	----	----

capsule was disassembled. An extremely large amount of wear debris was discovered even though the capsule was operated only for a very short running time. Apparently particles from the rings had become lodged between the assembly nut and the ball bearing housing, cutting deep grooves in the brass nut and producing more wear debris.

Another capsule was assembled using the gold-graphite ring cylinder. Preliminary evaluation again indicated that the capsule had unusually high drag-torque. When the brush block was removed, the drag-torque of the capsule decreased to a very low value in line with the expected drag-torque of the bearings. (Other measurements indicated that the typical drag-torque of the bearings used in the experimental capsules was 0.2 gm-cm.) The high drag-torque obtained with the gold-graphite composite ring cylinder was apparently due to the granular nature of the ring surface which resulted in a very high coefficient of friction between brush and ring, and which produced excessive amounts of wear debris after very short running times. Further evaluation of the gold-graphite system was not carried out.

VIII. SUMMARY AND CONCLUSIONS

The results of the experimental studies performed during this investigation have permitted the following general conclusions:

A. The rms and peak to peak electrical noise levels of miniature brush-ring systems are dependent upon the method used to drive the system during the noise measurements. Mechanically unbalanced drives produce high noise levels; balanced drives give lower levels; passive drives give the lowest levels.

B. The electrical noise exhibits a threshold effect with respect to the velocity of the sliding contact. For rotational systems, noise level is essentially constant for velocities above a specific value. During oscillation at constant frequency, noise level is essentially constant for deflection above a specific value.

C. Noise waveforms exhibit a strong tendency to repeat with respect to specific rotor position. This infers that noise spikes are associated with the surface condition at given angular positions of the ring.

D. Considerably lower noise levels than the presently accepted value of 10 microvolts per milliampere of brush current are possible with rings of soft gold, and soft gold with hard gold alloy overlays. Electroplated rhodium rings exhibit a noise level several times higher than those of the gold systems.

E. Run-in operations are effective in reducing noise level provided that a careful cleaning process follows the run-in. During run-in, extremely high noise levels are obtained. These are due

apparently to the formation of black deposits on the ring and brush surfaces. Inspection of the ring and brush surfaces after 100 hours of run-in and subsequent cleaning indicated very little permanent damage to the gold systems.

F. The major gases given off by epoxy resins at the lower pyrolysis temperatures are in the lower molecular weight range. Light gases such as hydrogen, carbon monoxide and methane are not believed to have a strong contamination potential because of their high mobility.

G. Contamination by creepage or exudation of material from epoxy insulations to the ring or brush surfaces is negligible.

H. If temperature differentials exist in the capsules, condensable products from epoxy insulations will be formed on the cold surfaces.

IX. RECOMMENDATIONS

Based upon the results of this investigation, it is recommended that the following activities be pursued in order to obtain a more complete understanding of miniature slip-ring problems.

- A. The general noise characteristics of vibration sensitivity, threshold effect, and repeatability should be verified by free oscillation and free rotation tests with commercially available slip-ring assemblies.
- B. Additional dielectric materials should be evaluated by the sublimation test, and the results correlated with processing and curing variables. The sublimation test should be refined to permit analysis of the condensate.
- C. The black deposits obtained during long term operation should be analyzed to determine their sources and also to permit specification of corrective measures. Based upon the limited wear effects that were observed, a large percentage of the objectionable deposits must be attributed to contaminant sources within the capsule. Whether deposits continue to accumulate after several run-in-cleaning cycles should also be determined.
- D. The effects of lubrication with synthetic oils should be determined. This includes both the effects on noise and wear and the effect on contamination potential of the insulations.

X. CONTRIBUTING PERSONNEL AND LOGBOOKS

Significant contributions to the over-all effort of this program were made by the following IITRI staff members:

Contamination Potential Of Insulations-R. E. Putscher, Research Chemist
Ring and Brush Materials-W.H. Graft, Research Metallurgist
Laboratory Evaluation-D. E. Richardson, Senior Electronic Engineer
Capsule and Apparatus Fabrication-J. J. Malin, Model Maker.

The detailed laboratory data of this investigation is contained in IITRI Logbooks C13395, C13984, C13994, C13995, C14251 and C14261.